UNIVERSIDADE FEDERAL DO RIO GRANDE DO SUL

PROGRAMA DE PÓS-GRADUAÇÃO EM CIÊNCIAS DA SAÚDE:

CARDIOLOGIA E CIÊNCIAS CARDIOVASCULARES

SERVIÇO DE CARDIOLOGIA DO HOSPITAL DE CLÍNICAS DE PORTO

ALEGRE

LABORATÓRIO DE FISIOPATOLOGIA DO EXERCÍCIO

DETERMINANTES DA FRAQUEZA E PROPRIEDADES CONTRÁTEIS DA MUSCULATURA INSPIRATÓRIA NA INSUFICIÊNCIA CARDÍACA

Aluna: Paula Aver Bretanha Ribeiro

Orientador: Prof. Dr. Jorge Pinto Ribeiro

Co-Orientador: Prof. Dr. Dilson Rassier

Agradecimentos

Durante esse período de formação acadêmica e pessoal, muitas pessoas foram importantes para que eu chegasse a esse momento, minha gratidão ficará aqui registrada.

Primeiramente, ao Prof Jorge Pinto Ribeiro, pela oportunidade, pelo exemplo de conduta acadêmica, pelo incentivo aos desafios e interesse pelas diferenças. Por me ensinar os caminhos para busca incessante pela melhor formação e pela verdade.

Ao meu co-orientador Prof Dilson Rassier, por me receber em seu laboratório em Montreal, Canadá e não medir esforços para que minha experiência fosse o mais produtiva possível, como de fato foi. Sem sua contribuição essa tese não teria sido possível.

À Profª. Beatriz Schaan, pela contribuição para minha formação acadêmica e profissional, as quais contribuíram para meu amadurecimento e oportunizaram parcerias que espero que se mantenham ao longo da minha vida acadêmica.

Ao PPG em Ciência da Saúde, representado pelos seus professores, por primar que profissionais com diversas formações em saúde tenham uma formação pautada pela excelência. À Sirlei, pela dedicação, amizade e cuidado com todos nós alunos do programa, meu muito obrigado.

Aos meus orientadores na minha Graduação e Mestrado, Prof Airton Rombaldi e Prof Eduardo Kokubun, esse trabalho tem muito da formação que também trago deles.

Aos colegas e amigos dos laboratórios brasileiro e canadense, pela amizade, parcerias produtivas e trocas que favoreceram meu aprendizado, em especial ao Daniel Umpierre, Paula Figueiredo, Marta Brod, Shana Grigoletti, Fabio Minozzo e Ivan Pavlov.

Aos amigos, que foram fundamentais em diversos momentos, de perto e/ou de longe, pelo acolhimento, por compartilharem risadas e lamentos, pelo aprendizado e por simplesmente caminharem ao meu lado. Alguns deles bem mais de perto e precisam ser mencionados: Daniele Vinholes, Daniele Massierer, Letícia Lobo, Glauco Pachalski e Lauriane Ginefri, muito obrigada com muito carinho.

Por final, à minha família, que sempre me apoiou, incentivou e alavancou a minha busca pelos meus sonhos. Por me darem o exemplo, pessoal e acadêmico, e me ensinarem que o crescimento pessoal perpasse pela boa educação, conduta ética, busca pela verdade e muito esforço. Em especial à minha mãe, que além de minha melhor amiga, lembra- me diariamente que os obstáculos aparecem à frente de quem caminha e que ao final todos valeram à pena.

SUMÁRIO

Lista de abreviaturas

FEVE – fração de ejeção do ventrículo esquerdo

FMI – fraqueza muscular inspiratória

FPM – fraqueza de preensão manual

IC – insuficiência cardíaca

ICC – insuficiência cardíaca crônica

PI_{max} – pressão inspiratória máxima

Resumo

A fraqueza muscular inspiratória pode estar presente em 30 a 50 % dos pacientes ambulatoriais com insuficiência cardíaca crônica, com implicações na qualidade de vida e prognóstico. Entretanto, não está claro quais características clínicas e comportamentais que estariam associadas a essa disfunção. Além disso, como não estão claros os mecanismos moleculares que conduzem a disfunção do diafragma. Parâmetros contráteis incluindo força de contração máxima, força passiva e cinética de pontes cruzadas podem estar alterados em pacientes com IC, e podem estar associados a FMI. Esta tese investigou, primeiramente, determinantes da FMI em comparação com a fraqueza muscular periférica (preensão manual), em pacientes com ICC. Neste estudo foram avaliadas variáveis clínicas, antropométricas e comportamentais destes pacientes. Os resultados demonstraram que apenas aproximadamente 50 % da FMI pode ser explicada pelas variáveis analisadas. Além disso, as variáveis associadas à fraqueza de preensão manual não são diferentes das encontradas em sujeitos saudáveis (gênero e idade). Entretanto, a força inspiratória máxima pode estar associada com marcadores de capacidade funcional do paciente. Em seguida, foram investigadas propriedades contráteis, ativas e passivas de miofibrilas de músculo cardíaco e diafragma, em um novo modelo animal de camundongos com insuficiência cardíaca desenvolvida por knockout para arginilação cardíaco-específica. Resultados do músculo cardíaco demonstram compatibilidade com a disfunção contrátil encontrada em humanos com insuficiência cardíaca congestiva, tais como redução da contração máxima, redução da força passiva e redução da cinética de relaxamento. Entretanto, nos resultados do músculo diafragma, encontramos aumento da força de contração máxima, o que pode sugerir uma mudança adaptativa compensatória associada ao aumento do trabalho inspiratório associado à insuficiência cardíaca crônica. Em conclusão, menos de 50 % da variância da força muscular inspiratória pode ser explicada por variáveis clínicas e comportamentais de pacientes com insuficiência cardíaca crônica. Em um modelo animal de insuficiência cardíaca que resulta em diminuição da contratilidade de cardiomiofibrilas, observa-se aumento da contratilidade das miofibrilas do diafragma, sugerindo que a fraqueza muscular inspiratória associada à insuficiência cardíaca crônica não seja secundária à disfunção contrátil da musculatura inspiratória.

Palavras-chave: insuficiência cardíaca; fraqueza muscular; biofísica muscular.

Abstract

The inspiratory muscle weakness may be present in 30-50% of outpatients with chronic heart failure, with implications for the quality of life and prognosis. However, it is unclear what clinical and behavioral characteristics that would be associated with this dysfunction. Moreover, as are unclear the molecular mechanisms leading to dysfunction of the diaphragm. Contractile parameters including contraction force maximum passive force and kinetics of cross-bridges can be altered in patients with HF, and may be associated with the IMF. This thesis investigated, firstly, the determinants of IMF in comparison to peripheral muscle weakness (handgrip) in patients with CHF. We evaluated clinical, anthropometric and behavioral disorders in these patients. The results showed that only about 50% of IMW can be explained by the variables. Furthermore, the variables associated with weakness of grip are not different from those found in healthy subjects (gender and age). However, maximum inspiratory force may be associated with markers of patient's functional capacity. Next, we investigated the contractile properties, assets and liabilities of myofibrils of cardiac muscle and diaphragm in an animal model of mice with heart failure developed by knockout arginilação cardiac-specific. Results show compatibility with the cardiac muscle contractile dysfunction found in human with congestive heart failure, such as reduction of maximum contraction, reduction and reduction of the passive force relaxation kinetics. However, the results of the diaphragm, we found increased maximum force of contraction, which may suggest a compensatory adaptive changes associated with increased inspiratory work associated with chronic heart failure. In conclusion, less than 50% of the variance in inspiratory muscle strength can be explained by behavioral and clinical variables of patients with chronic heart failure. In an animal model of heart failure that results in decreased contractility cardiomyofibrils, there was an increase in contractility of the diaphragm myofibrils, suggesting that inspiratory muscle weakness associated with chronic heart failure is not secondary to contractile dysfunction of the respiratory muscles.

Key words: heart failure; muscle weakness; muscle biophysics.

1. INTRODUÇÃO

A fraqueza muscular é um desfecho muito comum associado a diferentes condições clínicas. A redução da força muscular esquelética está diretamente associada à perda de independência, quedas, comprometimento das atividades da vida diária e, até mesmo, a mortalidade (Witham et al. 2006; Izawa et al 2009).

Dentre as manifestações clínicas decorrentes do comprometimento muscular, a fraqueza muscular inspiratória (FMI) tem ganho atenção especial (Chiappa et al.2008; Winkelman et al. 2009; Ribeiro et al 2009; Meyer et al. 2001). A FMI é encontrada em aproximadamente 30% dos pacientes ambulatoriais com insuficiência cardíaca (Chiappa et al.2008; Winkelman et al. 2009), e é resultado da redução da força dos músculos inspiratórios, principalmente do diafragma. Essa característica tem sido associada a sintomas como: dispnéia, percepção de fadiga crônica e intolerância ao exercício (Chiappa et al.2008; Winkelman et al. 2009; Wong et al. 2011; Stassijns et al. 1996).

Alguns mecanismos que conduzem à perda de força muscular esquelética foram sugeridos na literatura. Alguns estudos apontam a atrofia, a mudança para tipos de fibra I (Howell et al. 1995) e a perda de proteínas contrateis, como actina e titina (van Hees et al.2007; van Hees et al.2008; van Hees et al. 2010). Entretanto, o mecanismo que conduz especificamente a FMI ainda não está bem elucidado.

Portanto, esta tese apresenta, primeiramente, uma breve revisão de literatura que tenta estabelecer a relação entre fraqueza muscular inspiratória, fraqueza muscular periférica e propriedades contráteis envolvidas na disfunção muscular na insuficiência cardíaca. Em seguida, no estudo 1, apresenta uma análise transversal dos determinantes da fraqueza muscular inspiratória e fraqueza de preensão manual em pacientes com insuficiência cardíaca crônica, onde foram analisadas variáveis clínicas, antropométricas

e comportamentais destes pacientes. Nos dois estudos seguintes, apresenta análises das propriedades contráteis de músculo cardíaco e diafragma, de um novo modelo animal com insuficiência cardíaca em camundongos a partir de knockout para arginilação cardiomiócito específico.

2. REVISÃO DE LITERATURA

A Insuficiência Cardíaca (IC) é o desfecho final de várias doenças que acometem o coração, e é considerada um problema epidêmico em progressão (BOCCHI et al., 2009). É descrita com uma síndrome clínica complexa de caráter sistêmico, definida como disfunção cardíaca que ocasiona inadequado suprimento sangüíneo para atender as necessidades metabólicas tissulares, na presença de retorno venoso normal, ou fazê-lo somente com elevadas pressões de enchimento. Essa síndrome é o produto final de um processo, não só resultante de lesão miocárdica e sobrecarga hemodinâmica, mas também de ativação neuroumoral crônica e processos inflamatórios sistêmicos (Nobre & Serrano Jr, 2005). A redução do débito cardíaco é uma das manifestações hemodinâmicas mais comuns da IC, que leva a perfusão tecidual inapropriada, que se manifesta primeiramente durante o exercício e, com a progressão da doença, reduz o débito cardíaco também em repouso (Bocchi et al., 2009).

A IC pode ser resultado de disfunção sistólica, diastólica ou ambas. A fração de ejeção do ventrículo esquerdo (FEVE) é o índice mais utilizado para avaliar a função sistólica, e valores menores que 45-50% indicam disfunção, segundo as diretrizes européias (Dickstein et al., 2010). A disfunção diastólica caracterizada pela função sistólica preservada, mas presença de disfunção diastólica, que é definida pelo enchimento/relaxamento anormal (Bocchi et al. 2009).

A classificação da IC pode ser baseada em sintomas, proposta pela New York Heart Association (NYHA), desde a ausência de sintomas (classe I) até sintomas em repouso (classe IV). Os sintomas mais comuns da doença são dispnéia em esforços e

fadiga crônica, o que limita drasticamente a capacidade funcional e autonomia do paciente (BOCCHI et al., 2009).

2.1. Intolerância ao exercício e adaptações musculares na Insuficiência Cardíaca Crônica

Além da resposta anormal do débito cardíaco ao exercício, tem sido amplamente sugerido que fatores periféricos, localizados principalmente no músculo esquelético, são os principais determinantes da baixa tolerância ao esforço nestes indivíduos. Dentre eles: atrofia, mudança na distribuição entre os tipos de fibras musculares, alterações na relação entre os capilares sanguíneos e o músculo esquelético, que limitam a difusão de oxigênio do sangue para o tecido muscular e principalmente alterações intrínsecas do metabolismo muscular, que desencadeiam acidose e fadiga muscular precoce no exercício (Drexler, 1992; Wong et al. 2011).

A redução do fluxo sanguíneo muscular também é considerada, por alguns autores, um mecanismo fundamental na gênese da intolerância ao exercício na IC (Kubota et al. 1997; Richardson et al. 2003; Sullivan & Coob 1991). Chiba *et al*., (2007) demonstraram que pacientes com IC apresentam redução do fluxo sanguíneo muscular em resposta ao exercício e a diversos estímulos vasodilatadores. Classicamente, pacientes com IC apresentam diversas anormalidades na circulação periférica, advindas, entre outros, da importante ativação do sistema nervoso autônomo simpático (SNS) e também redução do fluxo sanguíneo muscular em repouso (Drexler et al, 1992). Acredita-se que o baixo aporte de oxigênio e a o excessivo aumento da resposta vasoconstritora, de forma crônica, sejam capazes de induzir a adaptações na musculatura esquelética periférica, e inclusive nos músculos respiratórios. Drexler et al. (1992) investigando as alterações na musculatura esquelética periférica de pacientes com ICC, encontraram uma redução de aproximadamente 20% da densidade

mitocondrial e densidade de superfície, além de redução na densidade capilar e uma maior transformação das fibras musculares para fibras tipo de IIb, em relação a controles saudáveis.

Algumas evidências ainda sugerem que as adaptações musculares em membros inferiores podem ser diferentes de membros superiores (ex. antebraço). Um estudo encontrou redução no desempenho de *endurance* no músculo do quadríceps femoral, mas não no adutor do polegar (Buller et al. 1991) quando usado protocolos de contração voluntária máxima e estimulação elétrica. Para estes achados o grupo especulou que a massa envolvida no exercício pode ser determinante no comprometimento muscular, portanto, pequenos grupamentos musculares não apresentariam comprometimento como os de grande grupamento muscular (ex. membros inferiores).

Entretanto, estudos sobre biofísica muscular para identificação das propriedades contráteis comprometidas na insuficiência cardíaca ainda são incomuns. Munkvik et al. (2011) avaliaram a força isométrica e isotônica em músculo esquelético periférico intacto de ratos com IC. O ponto chave deste estudo foi demonstrar que as contrações isométricas máximas são capazes de subestimar o comprometimento muscular, pois as contrações não permitem acessar o mecanismo de contração muscular no seu estado original (um ciclo após o outro) e mascaram índices de fadiga. Os resultados indicam que os músculos dos ratos com IC foram menos afetados pela fadiga, em contrações isotônicas seqüenciais, do que os músculos de ratos sham, achados que não corroboram com as evidências de que os músculos periféricos sofrem adaptações de transformação para fibras IIb (a qual seria menos resistente a fadiga), o que evidencia que o assunto ainda é controverso.

Okada et al. (2008) fizeram biópsia no vasto lateral de pacientes com insuficiência cardíaca crônica, após medidas de força de extensão de joelho e ergoespirometria. Apesar dos pacientes apresentarem redução na capacidade de exercício e na força de membros inferiores, avaliações *in vitro* de moléculas isoladas demonstraram que não existe alteração funcional nos filamentos finos (actina) ou filamentos grossos (miosina). Portanto, o comprometimento funcional no músculo *in vivo* deve ser atribuído a outros fatores, que não os de função molecular. Entretanto, esses resultados não avaliam o processo de contração muscular com a interação de todas as proteínas contráteis, a força passiva e a contribuição da titina no ciclo de contração muscular não foram avaliadas, o que não reproduz o processo fisiológico completo.

2.2. Fraqueza muscular inspiratória

A fraqueza muscular inspiratória (FMI) pode ser avaliada a partir da pressão inspiratória máxima (PI_{max}). A PI_{max} é mensurada a partir da pressão estática gerada na boca, durante esforços máximos de inspiração. Embora dependa do esforço do paciente, essa medida tem se mostrado confiável (McConnell & Copestake, 1999). Para fins clínicos, essa medida é bastante usada para acessar força global dos músculos inspiratórios, apesar de refletir, em maior magnitude, a força do músculo diafragma. Para determinação da fraqueza muscular inspiratória é utilizado o ponto de corte arbitrário de 70% da pressão inspiratória máxima predita para idade e sexo. Portanto, pacientes que apresentam a PI_{max} abaixo desse critério são classificados como portadores dessa fraqueza (D'allago et al. 2006; Ribeiro et al. 2009).

Em estudos do nosso laboratório, temos observado uma associação positiva entre a presença da FMI com capacidade de exercício reduzida (D'allago et al. 2006; Chiappa et al. 2008; Winkelman et al. 2009). Recentemente, demonstramos em nosso laboratório que baixos índices de força muscular inspiratória correlacionam-se diretamente com baixo consumo de oxigênio de pico no exercício, em pacientes com IC, e uma diminuição do fluxo sangüíneo dos músculos periféricos para os músculos inspiratórios mais acentuada, em relação aos pacientes sem fraqueza (Chiappa et al. 2008). Este fato pode ser justificado pelo excessivo aumento da resposta vasoconstritora, mediado pela ativação simpática quando aumentado a demanda dos músculos inspiratórios, mecanismo que pode ser responsável pela fadiga precoce dos músculos periféricos e que distingue os pacientes com FMI dos pacientes sem essa fraqueza.

A associação entre PI_{max} e prognóstico na ICC está bem descrita na literatura. A PI_{max} já se mostrou um forte preditor de risco de morte em pacientes com IC congestiva (Meyer et al. 2001) e não perdeu seu valor prognóstico mesmo na era do beta-bloqueadores (Frankenstein et al. 2009). Além disso, se associa positivamente com classe funcional (NYHA) e percepção de dispnéia (Ribeiro et al. 2009). Associa-se inversamente com resposta quimiorreflexa (Callegaro et al. 2010) e tem moderada correlação com consumo de oxigênio de pico (VO_2 de pico) (r = 0,32 – 0,59) (Ribeiro et al.2009).

Sabe-se que a FMI é reversível. Estudos que desenvolveram treinamento na musculatura inspiratória de paciente com ICC obtiveram resultados positivos. Dall`Ago et al. (2006), prescreveram um treinamento muscular inspiratório (TMI) de 12 semanas para pacientes com fraqueza muscular inspiratória, versos grupo placebo. Os resultados demonstraram melhora da PI_{max} em 115%, aumento de 17% no $VO_{2\ pico}$, além de melhora na qualidade de vida, melhora do teste de caminhada de 6 minutos.

Winkelmann et al. (2009) randomizaram pacientes para dois grupos de intervenção com exercício, um deles recebeu somente prescrição de exercício aeróbico, e o outro exercício aeróbico adicionado ao TMI. Os resultados desse estudo demonstraram que existe um ganho adicional quando o TMI é prescrito com treinamento aeróbico em relação ao $VO_{2\ pico}$ (21% x 41%, respectivamente). Chiappa et al. (2008) realizaram uma medida de espessura do diafragma, a qual serviu como medida adicional de disfunção do diafragma. Os resultados mostraram que, mesmo com somente 4 semanas de TMI, o diafragma responde com aumento significativo de espessura (59 ± 8 antes e 103 ± 16 após treinamento), e, além disso, o delta de espessura se associou significativamente com o delta na PI_{max} (r=0,88). Essa evidência suporta a teoria de que a FMI é reversível, não só na restituição da força, mas também na atrofia do diafragma.

Entretanto, as adaptações musculares no músculo diafragma, decorrentes da insuficiência cardíaca, parecem ser diferentes das adaptações ocorridas na musculatura esquelética periférica. Sabe-se que as fibras musculares tipo I e tipo IIa apresentam uma capacidade oxidativa maior em relação as fibras IIb. Tikunov et al. (1996) encontraram um aumento da proporção de fibras tipo I e IIa em diafragma de pacientes com IC crônica quando comparados com controle, indicando que existe uma adaptação muscular para aumentar a capacidade oxidativa desse músculo, que é comprovadamente comprometida na musculatura periférica (Drexler, et al. 1992; Filusch, et al. 2011; Stassijns et al. 1996).

De uma forma geral, a origem do declínio da força do músculo diafragma permanece controversa. Pode estar relacionado com mecanismos adaptativos da fisiopatologia da doença, como a diminuição de fibras tipo IIb; pode ser apenas uma conseqüência da atrofia causada pela redução do aporte de oxigênio para periferia, bem

como simplesmente desuso, pelo baixo nível de atividade física apresentado por esses pacientes, ou ainda, uma associação destes múltiplos fatores.

2.3. Músculo estriado e propriedades contráteis

O músculo estriado esquelético é uma estrutura complexa e altamente organizada. Regulado pelo sistema nervoso central, é composto de estruturas cilíndricas chamadas fibras musculares que se contraem homogeneamente. Cada fibra muscular também é composta de estruturas cilíndricas, denominadas miofibrilas, que são compostas de sarcômeros, estruturas organizadas em blocos longitudinais (Rassier, 2010). O sarcômero é a menor unidade funcional do músculo estriado, predominantemente composto de 3 diferentes moléculas: actina, miosina e titina. O processo contrátil se desenvolve principalmente pela interação dinâmica destas moléculas que desempenham funções distintas.

A actina é o componente protéico do filamento fino mais abundante, além dela, existem mais duas importantes proteínas a troponina e a tropomiosina. A troponina é a proteína que se liga ao cálcio e provoca o desvio da posição da tropomiosina para que libere o sitio ativo da actina, no qual a miosina se ligará, causando o que se chama de estado de ligação forte, o qual da inicio a contração na miofibrila. Já foram identificadas 6 isoformas dessa proteína, dentre elas a actina alfa 1, encontrada no músculo esquelético.

A miosina é o componente molecular do filamento grosso, considerada uma enzima mecanoquímica, pois converte a energia química (ATP) em mecânica (encurtando o sarcômero). A estrutura dessa molécula se constitui de uma cabeça, um

pescoço e uma cauda. A cabeça é onde se encontra o sítio de ligação para o ATP e com a actina; o pescoço que regula a atividade da cabeça por reação com outra proteína reguladora, a calmodulina; e a cauda que contém os sítios de ligação que vão determinar se essa proteína se liga a membrana plasmática ou a outras caudas para formação do filamento grosso. Esse filamento de miosina é constituído por duas cadeias pesadas de miosina e dois pares de cadeias leves de miosina. São as cadeias pesadas de miosina que carregam o sitio ativos do ATP e, por isso, determinantes pela taxa de consumo energético na contração miofibrilar. Essas cadeias apresentam duas isoformas, a alfa conhecida como miosina de cadeia pesada rápida (α MHC) que consome mais energia proveniente do ATP e desenvolve força mais rapidamente; e a beta conhecida como miosina de cadeia pesada lenta (β MHC), isoforma mais econômica e que desenvolve força mais lentamente (Hamdani et al., 2008).

A contração a nível miofibrilar se dá a partir da interação destas moléculas. O processo de contração se inicia com o impulso nervoso que atinge o reticulo sarcoplasmático e o cálcio é liberado. Em seguida, o cálcio se liga a troponina, que resulta em uma mudança de posição da tropomiosina, afastando-a dos sítios ativos da actina e permitindo que essa se ligue a miosina, em um "estado de ligação forte". A contração acontece em múltiplos ciclos desde que haja energia e cálcio livre disponível para se ligar a troponina. Quando a atividade nervosa cessa, o cálcio retorna ao retículo sarcoplasmático, o que faz a tropomiosina "cobrir" novamente os sítios ativos e provocar o relaxamento miofibrilar, nesse momento se estabelece um "estado de ligação fraco" entra a molécula de actina e a de miosina que se mantém até um novo estímulo de contração (Power & Howley, 2000).

A terceira proteína contrátil envolvida diretamente na contração muscular é a titina. A titina é conhecida como a proteína responsável pela elasticidade do sarcômero,

no modelo dos filamentos deslizantes da contração muscular. É a maior proteína encontrada nos mamíferos. No músculo humano é a maior proteína muscular em tamanho (massa mol 2700 - 4200 k Da, dependendo da isoforma) e em quantidade (8 – 10% do conteúdo muscular). É responsável pela expansão entre o disco Z e a linha M no sarcômero, e pela rigidez passiva do músculo. Além disso, a titina promove a sustentação, mantém a constituição muscular e exerce papel fundamental no desenvolvimento de força durante a contração muscular, além de ser um importante sensor mecânico (Figura A).

A titina trabalha como uma mola bidirecional que regula o comprimento do sarcômero e desempenha ajustes adequados na tensão passiva enquanto o movimento varia (Granzier & Labeit 2002; Wang, 1996; Ferreira, 2010).

Essa proteína é codificada por apenas um gene, localizado no cromossomo 2. A modulação da elasticidade/rigidez do segmento se dá através das diferentes isoformas expressadas no músculo esquelético (N2A), e no músculo cardíaco (N2B e N2AB) (Ferreira et al., 2010; Granzier & Labeit, 2002). A rigidez tende a se transformar ao longo da vida, adultos expressam isoformas mais responsivas ao Ca^{+} e isso torna o segmento mais rígido (Ottenheijm & Granzier, 2010). Os mecanismos que regulam a expressão gênica das isoformas da titina ainda são desconhecidos, sabe-se que cada patologia regula essas especificidades fenotípicas musculares de forma diferente.

Figura A. Esquema ilustrativo de sarcômero muscular. Linha preta central representa a linha M que se localiza no centro da banda A. Ligados a ele os filamentos grossos. Nas extremidades as linhas pretas representam a linha Z que estão no centro da banda I. Ligados a ele os filamentos finos e em diagonal (mais finos) os filamentos de titina.

Essa proteína é codificada por apenas um gene, localizado no cromossomo 2. A modulação da elasticidade/rigidez do segmento se dá através das diferentes isoformas expressadas no músculo esquelético (N2A), e no músculo cardíaco (N2B e N2AB) (Ferreira et al., 2010; Granzier & Labeit, 2002). A rigidez tende a se transformar ao longo da vida, adultos expressam isoformas mais responsivas ao Ca^{+} e isso torna o segmento mais rígido (Ottenheijm & Granzier, 2010). Os mecanismos que regulam a expressão gênica das isoformas da titina ainda são desconhecidos, sabe-se que cada patologia regula essas especificidades fenotípicas musculares de forma diferente.

2.3.1. Modelo das pontes cruzadas: teoria e delineamentos experimentais

A contração muscular é diretamente associada a Teoria das Pontes Cruzadas, originada por Huxley em 1957 e aceita pela comunidade cientifica até os dias de hoje. A teoria das pontes cruzadas propõe que o encurtamento e a força produzidos em um músculo ocorrem como resultado da interação de duas proteínas contráteis: actina e miosina. A miosina tem uma protrusão (ponte-cruzada) que ciclicamente se acopla a actina e a move na direção do centro do sarcômero. Apesar de uma teoria simplificada, a propriedades básicas do modelo das pontes-cruzadas tem se mantido ao longo das descobertas na área.

O modelo das pontes cruzadas pode ser descrita em dois estados, quando as pontes cruzadas estão ligadas ou separadas da actina. No modelo original proposto por Huxley (1957), duas taxas constantes foram usados para descrever a transição entre os dois estados: f , a taxa de pontes cruzadas ligadas a actina, e g , a taxa de pontes cruzadas separadas da actina (Huxley, 1957). O modelo assume que (i) cada ponte cruzada tem um componente elástico; (ii) a probabilidade das pontes cruzadas se ligarem a actina, que resulta em força do componente elástico, é moderada; e (iii)

quando as pontes cruzadas aumentam a tensão, a probabilidade de separar da actina é baixa. A equação que explica o número de pontes cruzadas é dada por:

$$n(\infty) = \frac{f}{f+g}$$

Portanto, o número de pontes cruzadas ligadas a actina (n) num dado momento (em equilíbrio ou steady-state) será regulada pela probabilidade de ligação e separação entre as cabeças de miosina e a actina (Huxley, 1957).

2.3.2. Estudos experimentais que avaliam a cinética das pontes cruzadas

Avaliar o modelo de pontes cruzadas e as constantes cinéticas, incluindo as constantes de ligação e dissociação, ciclo de pontes cruzadas e a geração de força pelo músculo, é complexo. Uma das metodologias que tem sido utilizada com sucesso na área da biofísica muscular envolve estudos delineados para avaliar as taxas de desenvolvimento e redesenvolvimento de força e relaxamento ativados por cálcio, em amostras musculares, sejam elas em fibras permeabilizadas (van Hees et al. 2007) ou feixes de miofibrilas (Kurosaka et al. 2012).

2.3.3. Desenvolvimento e redesenvolvimento de força

A taxa de desenvolvimento de força sobre ativação muscular provém informação sobre os efeitos da regulação de Ca^{2+} e taxas correspondente da formação e ciclo das pontes cruzadas. Desde que a ponte cruzada inicie, no estado separado da actina, a taxa de desenvolvimento de força fornece informação sobre o quanto rápido as pontes cruzadas se ligam a actina ciclicamente até que a força estabilize. Naturalmente, sobre estas circunstâncias a cinética das pontes cruzadas não são separadas do efeito da regulação do Ca^{2+} no filamento fino, o qual é importante para entender a regulação

muscular, mas representa uma limitação se o objetivo da investigação for entender a cinética das pontes cruzadas. Para superar essa limitação, um protocolo mecânico foi desenvolvido para estudar a taxa de redesenvolvimento de força (Brenner and Eisenberg, 1986). Sob ativação máxima, fibras musculares foram submetidas ao encurtamento induzido mecanicamente seguido de um rápido alongamento ao comprimento de sarcômero original. Tem sido estimado que esse procedimento separada de 80-90% das pontes cruzadas durante do encurtamento, e o redesenvolvimento de força pode assumir ativação em constante [Ca^{2+}] – sem interferência dos processos regulatório do Ca^{2+}. Após o encurtamento e realongamento, com a maioria das pontes cruzadas em estado separado da actina, as remanescentes estarão ligadas em estado de ligação fraca a actina. Como resultado, a cinética de redesenvolvimento (K_{tr}) descreve a rápida religação das pontes cruzadas e subsequente transição para um estado forte de ligação. Portanto, os efeitos da regulação do Ca^{2+} e a cinética das pontes cruzadas podem ser examinados sem a preocupação dos efeitos advindos do comprimento de sarcômero (o comprimento é o mesmo antes e depois do encurtamento), sobreposição dos filamentos, e regulação de Ca^{2+} (Brenner 1988; Brenner et al. 1998).

Usando esse protocolo, a taxa de desenvolvimento de força inicial sob ativação muscular, redesenvolvimento de força após o procedimento de encurtamento e realongamento e o relaxamento são aproximados com funções mono ou bi-exponenciais (Araujo & Walker 1994; Brenner 1988; Brenner & Eisenberg 1986; Fitzsimons et al. 1998; Gordon et al. 2000; Millar & Homsher 1990; Palmer & Kentish 1998; Stehle et al. 2009; Wolff et al. 1995). Usando as constantes de tempo destas equações, é possivel determinar as taxas constantes que governam esses fenômenos, como a seguir:

$$F(t) = A(1 - e^{-kt}) + B$$

Onde *F* é a força (em função do tempo), *t* é tempo, *k* é a taxa constante exponencial e *A* e *B* são constantes.

Durante o desenvolvimento inicial de força, a ligação do Ca^{2+} a troponina-C inicia um deslocamento da posição da tropomiosina, o qual permite as pontes cruzadas se ligarem ao filamento de actina, os quais são descritos pela constante cinética K_{act}. Durante o redesenvolvimento de força, o Ca^{2+} já está presente e o deslocamento da tropomiosina se presume que já tenha acontecido, portanto, de acordo com o modelo "steric" para regulação muscular o valor de K_{tr} é estimado para ser maior que K_{act}. A regulação por Ca^{2+} ocorre rápido suficiente para que não ocorra efeito de "rate-limiting" nos valores de K_{act} ou K_{tr} (Bell et al. 2006; Solzin et al. 2007; Stehle et al. 2009). Na ativação máxima estável de Ca^{2+}, a taxa máxima do turnover de pontes cruzadas é dada por: $f + g$. A taxa constante para uma equação mono-exponencial descreve o número de pontes cruzadas na

$$n(t) = \frac{f}{f+g}\left(1 - e^{-(f+g)t}\right)$$

com marcada similaridade com o modelo original de pontes cruzadas.

2.3.4. Relaxamento Muscular

A cinética do relaxamento muscular tem sido usada para avaliar a separação das pontes cruzadas da actina, que pode ser descrita de forma bifásica com um componente lento linear (K_{lin}) e componente rápido exponencial (K_{rel}) (Poggesi et al. 2005; Stehle et al. 2002a; Stehle et al. 2002b; Tesi et al. 2002b). O componente exponencial é tipicamente caracterizado por uma equação mono-exponencial com a taxa constante K_{rel}.

Em geral, o relaxamento muscular acontece principalmente pelo desligamento das pontes cruzadas, com pequeno atraso no início do deslizamento dos filamentos para trás (deslizando na direção oposta da ativação) (Stehle et al. 2002a) (Piroddi et al. 2007; Poggesi et al. 2005; Tesi et al. 2002b). Com a diminuição da concentração do Ca^{2+} durante o relaxamento, as pontes cruzadas de miosina se separarão em uma taxa *g* com diminuição da probabilidade de reconectar (Brenner 1988; Stehle et al. 2009). De fato, vários estudos sugerem que $K_{lin} \approx g$ (Poggesi et al. 2005; Stehle et al. 2002a; Tesi et al. 2002a); a fase linear do relaxamento está diretamente associada com a desconexão das pontes cruzadas. Como o número de pontes cruzadas desconectadas aumenta, as pontes cruzadas remanescentes conectadas a actina estariam sujeitas a maior tensão e seria mais provável para separar (Stehle et al. 2009; Tesi et al. 2002b). Como o relaxamento continua e a tensão aumenta para as pontes cruzadas, estas estarão mais propensas a sofrer uma inversão do "power-stroke", envolvendo a captação de Pi e descolamento posterior (Lipscomb et al 1999;. Shirakawa et al 2000;. Simnett et al 1998; Stehle et al, 2002a; Tesi et al. 2002a). Concomitantemente, a liberação de tensão também promove maior separação ponte cruzada, esse processo facilitaria a ligação de ATP para a miosina e desprendimento de actina (Stehle et al, 2002a; Stehle et al 2009; Tesi et al, 2002a.).

2.4. Propriedades contráteis do músculo estriado cardíaco e diafragma

Nos últimos anos, diferentes estudos têm sido conduzidos a fim de evidenciar os mecanismos regulatórios das propriedades contráteis. Estudos realizados em músculo cardíaco de humanos com doença cardíaca isquêmica demonstraram modificação na isoforma da titina, como resultado de remodelamento muscular. Neagoe et al. (2002) demonstraram um aumento da expressão da isoforma mais complacente da titina (N2BA), a qual seria em resposta ao aumento da rigidez das paredes do ventrículo

esquerdo, causado pelo aumento de colágeno e desmina, em pacientes com diagnóstico de doença isquêmica não recente. Entende-se essa alteração da expressão das isoformas como um mecanismo compensatório celular, o que pode indicar que a titina não participa do mecanismo de rigidez do ventrículo esquerdo nestes pacientes, pois o mesmo não foi evidenciado em corações normais.

Estudos realizados com fibras isoladas de diafragmas de ratos com IC demonstraram a diminuição da tensão gerada no músculo em aproximadamente 35%, entretanto quando avaliado o músculo sóleo essa diferença não se confirmou. Os autores atribuíram essa redução da força a redução de 25% no conteúdo de titina diafragmática, apesar do tamanho dessa proteína não ter sofrido modificações (van Hees et al., 2010). O mesmo grupo conduziu experimentos em fibras isoladas do diafragma de pacientes com IC congestiva e encontraram um decréscimo na força isométrica máxima e submáxima, além do decréscimo da potência máxima de aproximadamente 35% em relação aos ratos controle e a redução da máxima velocidade de encurtamento. Entretanto, o sarcolema dos ratos demonstrou-se intacto, demonstrando que a disfunção muscular não está relacionada a esta membrana.

Lange et al. (2005) investigaram o desuso no músculo diafragma e encontraram uma remodelação adaptativa, com decréscimo de conteúdo de titina e diminuição da sensibilidade ao Ca+, resultado da expansão do espaço interfilamentos que afeta o acoplamento da miosina no filamento fino. Por conseqüência, ocorre diminuição da síntese protéica pela diminuição de carga no filamento grosso. Além disso, os autores sugerem que deformações da banda M durante o alongamento ou contração muscular podem estar envolvidas na sinalização do domínio da protein kinase, que pode ser modulada por estas mudanças conformacionais.

3. REFERÊNCIAS

1. Araujo A, Walker JW. Kinetics of tension development in skinned cardiac myocytes measured by photorelease of Ca2+. Am J Physiol.267(5 Pt 2):H1643-53, 1994.

2. Bell CJ, Bright NA, Rutter GA, Griffiths EJ. ATP regulation in adult rat cardiomyocytes: time-resolved decoding of rapid mitochondrial calcium spiking imaged with targeted photoproteins. J Biol Chem. 22;281(38):28058-67, 2006.

3. Bocchi EA, Marcondes-Braga FG, Ayub-Ferreira SM, Rohde LE, Oliveira WA, Almeida DR, e cols. Sociedade Brasileira de Cardiologia. III Diretriz Brasileira de Insuficiência Cardíaca Crônica. Arq Bras Cardiol 93(1 supl.1):1-71, 2009.

4. Brenner B, Eisenberg E. Rate of force generation in muscle: correlation with actomyosin ATPase activity in solution. Proc Natl Acad Sci U S A. 83(10):3542-6, 1986.

5. Brenner B. Effect of Ca2+ on cross-bridge turnover kinetics in skinned single rabbit psoas fibers: implications for regulation of muscle contraction. Proc Natl Acad Sci U S A.85(9):3265-9, 1988 .

6. Brenner B, Kraft T, Chalovich JM. Fluorescence of NBD-labelled troponin-I as a probe for the kinetics of thin filament activation in skeletal muscle fibers. Adv Exp Med Biol.453:177-84, 1998.

7. Buller, NP ; Jones, D ; Poole-Wilson, PA. Direct measument of skeletal muscle fatigue in patiens with chronic heart failure. Br Heart J 65 :20-24, 1991.

8. Callegaro CC, Martinez D, Ribeiro PA, Brod M, Ribeiro JP.Augmented peripheral chemoreflex in patients with heart failure and inspiratory muscle weakness. Respir Physiol Neurobiol. 2010 Apr 15;171(1):31-5.

9. Chiappa GR, Roseguini BT, Vieira PJ, Alves CN, et al. Inspiratory muscle training improves distribution of blood flow to resting and exercising limbs in patients with chronic heart failure. J Am Coll Cardiol. 51(17):1663-71, 2008.

10. Chiba Y, Maehara K, Yaoita H, Yoshihisa A, Izumida J, Maruyama Y. Vasoconstrictive Response in the Vascular Beds of the Non-Exercising Forearm During Leg Exercise in Patients With Mild Chronic Heart Failure. Circ J 71: 922 –928, 2007.

11. Dall'Ago P, Chiappa GR, Guths H, Stein R, Ribeiro JP. Inspiratory muscle training in patients with heart failure and inspiratory muscle weakness: a randomized trial. J Am Coll Cardiol. 47: 757-63, 2006.

12. Dickstein, K et al. Focused update on device therapy in heart failure. European Heart Journal 31: 2677-2687, 2010.

13. Drexler H, Riede U, Munzel T, Konig H, Funke E, Just H. Alterations of skeletal muscle in chronic heart failure. Circulation 85: 1751-1759, 1992.

14. Ferreira RC, Carvalho RF, Pires IF, Moreira AL. The role of titin in the modulation of cardiac function and its pathophysiological implications. Arq Bras Cardiol 96 (4): 332-339, 2011.

15. Filush A, Ewert R, Altesellmeier M, Zugck C, Hetzer R, Borst MM, Katus HA, Meyer FJ. Respiratory muscle dysfunction in congestive heart failure – the role of pulmonary hypertension. Int J Cardiol 150: 182-185, 2011.
16. Frankenstein L, Nelles M, Meyer J, Sigg C, Schellberg D, Remppis A, Katus HA, Zugck C. Validity, prognostic value and optimal cutoff of respiratory muscle strength in patiens with chronic heart failure changes with beta-blocker treatment. Eur J Cardiovasc Prev Rehabil 16:424-429, 2009.
17. Gordon AM, Homsher E, Regnier M. Regulation of contraction in striated muscle. Physiol Rev.80(2):853-924, 2000.
18. Granzier H, Labeit, S. Cardiac titin: na adjustable multi-functional spring. Journal of Physiology, 541, pp 335-342, 2002.
19. Hamdani N, Kooij V, van Dijk S, Merkus D, Paulus WJ, Remedios CD, Duncker DJ, Stienen GJ, van der Velden J Sarcomeric dysfunction in heart failure. Cardiovasc Res. 1;77(4):649-58, 2008.
20. Huxley AF. Muscle structure and theories of contraction. Prog Biophys Biophys Chem.7:255-318 1957.
21. Izawa KP, Watanabe S, Osadab N, Kasaharaa Y, Yokoyama H, Hirakia K, Morioa Y, Yoshiokaa S, Okac K, Omiyab K. Handgrip strength as a predictor of prognosis in Japanese patients with congestive heart failure. European Journal of Cardiovascular Prevention and Rehabilitation 16:21–27, 2009.
22. Kurosaka S, Leu NA, Pavlov I, Han X, Ribeiro PA, Xu T, Bunte R, Saha S, Wang J, Cornachione A, Mai W, Yates JR 3rd, Rassier DE, Kashina A. Arginylation regulates myofibrils to maintain heart function and prevent dilated cardiomyopathy. J Mol Cell Cardiol. 2012 [Epub ahead of print].
23. Kubota T, Imaizumi T, Oyama J, Ando S, Takeshita A. L-arginine increases exercise induced vasodilation of the forearm in patients with heart failure. Jpn Circ J 61:471-480, 1997.
24. Lange S, Xiang F, Yakovenko A et al. The kinase domain of titin controls muscle gene expression and protein turnover. Science 308, 1599, 2005.
25. Lipscomb S, Palmer RE, Li Q, Allhouse LD, Miller T, Potter JD, Ashley CC. A diazo-2 study of relaxation mechanisms in frog and barnacle muscle fibres: effects of pH, MgADP, and inorganic phosphate. Pflugers Arch. 1999 Jan;437(2):204-12.
26. McConnell AK, Copestake AJ. Maximum static respiratory pressures in healthy elderly men and women: issues about reproducibility and interpretation. Respiration 66:251-258, 1999.
27. Meyer FJ, Borst MM, Zugck C, Kirschke A, Schellberg D, Kübler W, Haass M. Respiratory Muscle Dysfunction in Congestive Heart Failure. Circulation 103:2153-2158, 2001.
28. Millar NC, Homsher E. The effect of phosphate and calcium on force generation in glycerinated rabbit skeletal muscle fibers. A steady-state and transient kinetic study. J Biol Chem. 1990 Nov 25;265(33):20234-40.
29. Munkvik M, Lunde PK, Aronsen JA, Birkeland JAK, Sjaastad I, Sejersted OL. Attenuated fatigue in slow twich skeletal muscle during isotonic exercise in rats with chronic heart failure. PLoS one, v. 6 (7), 2011.

30. Neagoe C, Kulke M, del Monte F, Gwathmey JK, de Tombe PP, Hajjar RJ, Linke WA.et al. Titin isoform switch in ischemic human heart disease. Circulation 106: 1333-1341, 2002.
31. Nobre F, Serrano Jr CV. Editores: Tratado de Cardiologia SOCESP. Barueri, SP: Manole, 2005.
32. Okada Y, Toth MJ, VanBuren P. Skeletal muscle contractile protein function is preserved in human heart failure. J Appl Physiol 104:952-957, 2008.
33. Ottenheijm CAC, Granzier H. Role of titin in skeletal muscle function and disease. In: Muscle Biophysics: from molecules to cells. Adv Experim Med Biol, v. 682, 2010.
34. Palmer S, Kentish JC. Roles of Ca2+ and crossbridge kinetics in determining the maximum rates of Ca2+ activation and relaxation in rat and guinea pig skinned trabeculae. Circ Res. 27;83(2):179-86, 1998.
35. Piroddi N, Belus A, Scellini B, Tesi C, Giunti G, Cerbai E, Mugelli A, Poggesi C. Tension generation and relaxation in single myofibrils from human atrial and ventricular myocardium. Pflugers Arch.454(1):63-73, 2007.
36. Poggesi C, Tesi C, Stehle R. Sarcomeric determinants of striated muscle relaxation kinetics. Pflugers Arch.449(6):505-17, 2005.
37. Rassier D. Striated muscles: from molecules to cells. In: Muscle Biophysics: from molecules to cells. Adv Experim Med Biol, v. 682, 2010.
38. Ribeiro JP, Chiappa GR, Neder JA, Frankenstein L. Respiratory muscle function and exercise intolerance in heart failure. Curr Heart Fail Rep. 6(2):95-101, 2009.
39. Richardson T, Kindig C, Musch T, Poole D. Effects of chronic heart failure on skeletal muscle capillary hemodynamics at rest and during contractions. J Appl Physiol 95:1055-1602, 2003.
40. Simnett SJ, Johns EC, Lipscomb S, Mulligan IP, Ashley CC. Effect of pH, phosphate, and ADP on relaxation of myocardium after photolysis of diazo 2. Am J Physiol. 275(3 Pt 2):H951-60, 1998.
41. Solzin J, Iorga B, Sierakowski E, Gomez Alcazar DP, Ruess DF, Kubacki T, Zittrich S, Blaudeck N, Pfitzer G, Stehle R. Kinetic mechanism of the Ca2+-dependent switch-on and switch-off of cardiac troponin in myofibrils. Biophys J. 1;93(11):3917-31 2007.
42. Stassijns G, Lysens R, Decramer M. Peripheral and respiratory muscles in chronic heart failure. Eur Respir J. 9(10):2161-7, 1996.
43. Stehle R, Krüger M, Scherer P, Brixius K, Schwinger RH, Pfitzer G. Isometric force kinetics upon rapid activation and relaxation of mouse, guinea pig and human heart muscle studied on the subcellular myofibrillar level. Basic Res Cardiol. 97 Suppl 1:I127-35, 2002.
44. Stehle R, Solzin J, Iorga B, Poggesi C. Insights into the kinetics of Ca2+-regulated contraction and relaxation from myofibril studies. Pflugers Arch.458:337-57, 2009.
45. Sullivan M, Cobb F. Dynamic regulation of leg vasomotor tone in patients with chronic heart failure. J Appl Physiol 71:1070-1075, 1991.

46. Tikunov BA, Mancini D, Levine S. Changes in Myofibrillar protein composition of human diaphragm elicited by congestive heart failure. J Mol Cell Cardiol 28: 2537-2541, 1996.
47. van Hees HWH, Ottenheijm CAC, Granzier HL, Dekhuijzen PNR, Heunks LMA. Heart failure decreases passive tension generation of rat diaphragm fibers. International Journal of Cardiology, 141, pp 275-283, 2010.
48. van Hees HWH, van der Heijden HFM, Hafmans T, Ennen L, Heunks LMA, Verheugt FWA, Dekhuijzen PNR. Impaired isotonic contractility and structural abnormalities in the diaphragm of congestive heart failure rats. International Journal of Cardiology, 128, pp- 326-335, 2008.
49. van Hees HWH, van der Heijden HFM, Ottenheijm CAC, Heunks LMA, Pigmans CJC, Verheugt FWA, Brouwer RMHJ, Dekhuijzen PNR. Diaphragm single-fiber weakness and loss of myosin in congestive heart failure rats. Am J Physiol Heart Circ Physiol, 293, pp H819-H828, 2007.
50. Wang, K. Titin/connectin and nebulin: giant protein rules of muscle structure and function. Adv. Biophys., Vol.33, pp 123-134, 1996.
51. Winkelmann E, Chiappa GR, Lima COC, Viecili PRN, Stein R, Ribeiro JP. Addition of Inspiratory Muscle Training to Aerobic Training Improves Cardiorespiratory Responses to Exercise in Patients with Heart Failure and Inspiratory Muscle Weakness. The American Heart Journal, 158:768.e1-768.e7, 2009.
52. Witham M, Argo I, Johnston D, Struthers AD, McMurdo MET. Predictors of exercise capacity and everyday activity in older heart failure patients. The European Journal of Heart Failure 8: 203 – 207, 2006.
53. Wong E, Selig S, Hare DL. Respiratory muscle dysfunction and training in chronic heart failure. Heart, Lung and Circulation 20:289-294, 2011.

4. JUSTIFICATIVA

A associação entre fraqueza muscular inspiratória (FMI) e prognóstico na IC está descrita na literatura. Entretanto, não está claro quais características clínicas e comportamentais que estariam associadas a essa disfunção, o que permitiria intervir diretamente nos determinantes da FMI, característica que está presente em 30 - 50% dos pacientes ambulatoriais na IC. Além disso, não se sabe o quanto a FMI reflete a possível disfunção do diafragma. Parâmetros contráteis incluindo força de contração máxima, força passiva e cinética de pontes cruzadas podem estar alterados em pacientes com IC, e podem estar associados a FMI.

Para tanto, esta tese investigou primeiramente determinantes da fraqueza muscular inspiratória em comparação com a fraqueza periférica, aferida através de preensão manual, em pacientes com insuficiência cardíaca crônica. Neste estudo foram utilizadas variáveis clínicas, antropométricas e comportamentais destes pacientes. Os resultados demonstraram que apenas aproximadamente 50 % da FMI pode ser explicada por estas variáveis. Estes resultados nos motivaram a direcionar os próximos estudos desta tese a investigação de mecanismos intracelulares envolvidos na geração de força. Para tanto, foram investigadas propriedades contráteis, ativas e passivas de miofibrilas de músculo cardíaco e diafragma, em um novo modelo animal de camundongos com insuficiência cardíaca desenvolvida por knockout para arginilação específica para cardiomiócito. A utilização de experimentos com miofibrilas isoladas destes camundongos permitiu a análise da menor unidade contrátil do músculo estriado que ainda mantém a estrutura tri-dimensional com todas as proteínas contrateis intactas, permitindo a avaliação direta dos da cinética das pontes cruzadas usando-se como

indicadores a taxa de desenvolvimento de força, taxa de redesenvolvimento de força e relaxamento, como explicado anteriormente nesta tese.

5. OBJETIVOS

5.1. Gerais

Estudo 1: Avaliar a relação entre variáveis clínicas, antropométricas e comportamentais, pressão inspiratória máxima e força de preensão manual em pacientes ambulatoriais com insuficiência cardíaca crônica.

Estudo 2: Avaliar as propriedades contráteis miofibrilares do músculo cardíaco de camundongos com insuficiência cardíaca desenvolvida a partir de um modelo de knockout para arginilzação cardiomiocito-específico.

Estudo 3: Avaliar as propriedades contráteis miofibrilares do diafragma de camundongos com insuficiência cardíaca desenvolvida a partir de um modelo de knockout para arginilzação cardiomiocito-específico.

5.2. ESPECÍFICOS

Estudo 1:

a) Avaliar a prevalência da fraqueza muscular inspiratória e seus determinantes clínicos e comportamentais, em pacientes ambulatoriais com insuficiência cardíaca crônica;

b) Avaliar a prevalência da fraqueza de preensão manual e seus determinantes clínicos e comportamentais, em pacientes ambulatoriais com insuficiência cardíaca crônica;

c) Comparar os determinantes da fraqueza muscular inspiratória com os determinantes da fraqueza de preensão manual.

Estudo 2:

a) Avaliar as seguintes propriedades contráteis miofibrilares de músculo cardíaco de camundongos com insuficiência cardíaca e comparar com camundongos controle saudáveis.

(i) força máxima, em diferentes comprimentos de sarcômero, normalizada pela secção transversal;

(ii) taxa de desenvolvimento e redesenvolvimento de força;

(iii) taxa de relaxamento;

(iv) força passiva, em diferentes comprimentos de sarcômero, normalizada pela secção transversal.

Estudo 3:

a) Avaliar as seguintes propriedades contráteis miofibrilares do músculo diafragma de camundongos com insuficiência cardíaca e comparar com camundongos controle saudáveis.

(i) força máxima, em diferentes comprimentos de sarcômero, normalizada pela secção transversal;

(ii) taxa de desenvolvimento e redesenvolvimento de força;

(iii) taxa de relaxamento;

(iv) força passiva, em diferentes comprimentos de sarcômero, normalizada pela secção transversal.

ARTIGO I

Determinants of handgrip and inspiratory muscle strength in chronic heart failure

Determinantes da força de preensão manual e músculos inspiratórios na insuficiência cardíaca crônica

Determinants of handgrip and inspiratory muscle strength in chronic heart failure

Paula A. B. Ribeiro[1]; Marta S. Brod[1,2]; Daniele B. Vinholes[3]; Jorge P. Ribeiro[1,4]

[1] Exercise Pathophysiology Research Laboratory and Cardiology Division, Hospital de Clínicas de Porto Alegre, Universidade Federal do Rio Grande do Sul , Brazil
[2] Faculdades Atlântico Sul, Rio Grande, Brazil.
[3] Universidade do Sul de Santa Catarina, Tubarão, Brazil.
[4] Department of Medicine, Faculty of Medicine, Federal University Rio Grande do Sul, Porto Alegre, Brazil

Abstract

Background: In patients with chronic heart failure, respiratory and peripheral muscle weakness is common and is associated with the severity of disease as well as prognosis. However, the determinants of these muscle dysfunctions are not clear. To better understand determinants and correlates of these conditions, we conducted a cross-sectional study in an ambulatory sample of patients with chronic heart failure. **Methods and Results:** Fifty one patients underwent evaluation of maximal inspiratory muscle pressure (PI_{max}), handgrip strength, anthropometric measures, functional capacity, self-reported physical activity, objectively-measured physical activity, depression scale, quality of life, and clinical evaluations. The prevalence of handgrip weakness was higher (78%) than inspiratory muscle weakness (41%). In univariate analysis, variables that correlated with handgrip strength were: gender, functional capacity (NYHA), six minute walk test (6MWT), peak oxygen uptake (VO_{2peak}), PI_{max}, and emotional score from the Minnesota Living with Heart Failure Questionnaire (MLHF). In univariate analysis, variables that correlated with PI_{max} were: years of schooling, NYHA, handgrip, and emotional score from MLHF. In multivariate analysis, age, gender, and PI_{max} were independent predictors for handgrip strength. In multivariate analysis, physical score of MLHF, schooling and handgrip strength were independent predictors for PI_{max}. The multivariable models predicted poorly handgrip strength ($r^2 = 0.45$, $p < 0.01$) and PI_{max} ($r^2 = 0.40$, $p < 0.01$). **Conclusions:** We found different correlates for peripheral and inspiratory muscle weakness. Since only about 40-45 % of handgrip and inspiratory muscle strength variance can be accounted for by the variables here evaluated, future studies should be conducted to identify other determinants in this patient population.

Key words: heart failure; muscle weakness; respiratory muscles; muscle strength; physical activity

Introduction

Patients with chronic heart failure (CHF) may have some impairment in the performance of everyday tasks. Dyspnea and chronic fatigue are symptoms that limit effort on daily life activities and regular physical activity (PA). This disability may be influenced by peripheral and inspiratory muscle weaknesses, which are common in this patient population[1,2,3]. In CHF patients, the underlying mechanisms that lead to this process have only been partially elucidated. The muscular condition seems to be independent of central hemodynamics, as previously demonstrated[4], and improvements in hemodynamic parameters do not necessarily reverse muscular impairment. Moreover, physical training improves this muscle condition without any changes in central hemodynamic function[5,6].

A previous study demonstrated that handgrip strength is more impaired than inspiratory strength in CHF[7]. On the other hand, inspiratory muscle strength,

accessed by maximal inspiratory pressure (PI_{max}), did not correlate with quadriceps strength[8]. However, it is still not clear what determines respiratory and peripheral skeletal muscle strength in CHF. This muscle weakness has been associated with cachexia and sarcopenia[6] or may be a consequence of age, disuse or a sedentary life style[9,10,11]. Since physical training improves inspiratory and peripheral muscle weakness[5,6,12], the reduced physical activity during daily living has been suggested as one of the determinants of muscle weakness in CHF. To better understand determinants and correlates of inspiratory and peripheral muscle strength, we conducted a cross-sectional study in an ambulatory sample of patients with CHF.

Methods

Protocol. Eligible patients were recruited from the Heart Failure Clinic of the Hospital de Clínicas Porto Alegre. They were initially evaluated by medical history, physical examination, inspiratory muscle and handgrip strength. After that they were invited to visit the hospital two times more to perform cardiopulmonary test and accelerometer measurements.

Patients. Inclusion criteria were stable chronic heart failure due to systolic dysfunction (left ventricular ejection fraction < 45%) or with preserved systolic function (left ventricular ejection fraction > 45%)[13]. Exclusion criteria were history of pulmonary disease, current smoking, angina, recent surgery or infarction (<6 months), orthopaedic or neurological impairment, or cancer chemotherapy. The protocol was approved by ethical committee the institution and all patients assigned an informed consent form.

Clinical characteristics. Age, left ventricular ejection fraction (by echocardiography), and heart failure etiology were obtained from hospital records. Additional information was obtained with semi-structured questionnaire about socioeconomic status and use of medication. Body mass index (BMI) was calculated using the formula weight (kg) / height^2 (m).

Inspiratory muscle strength. PI_{max} was measured as previously described, using a pressure transducer (MVD-550, V 11 Microhard System, Globalmed, Porto Alegre, Brazil)[14]. Inspiratory muscle weakness was defined as a PI_{max} of less than 70 % of predicted[1,15]. The best of 6 tests was chosen to represent PI_{max}.

Handgrip strength. Handgrip was used as general muscle strength. To measured and calculate weakness, we used a hydraulic hand dinamometer - Jamar® (Sammons Preston, Bolingbrook, IL, USA). Maximal force of 3 tests with both hands was evaluated. The strength index was a mean of best try of dominant hand and cut-point of weakness (32.2 Kgf[16]) was age and gender predicted[17].

Cardiopulmonary exercise testing. Patients underwent symptom-limited testing on a treadmill (IMBRAMED, Brazil) using a ramp protocol, until exhaustion, as previously described[18]. In short, breath-by-breath gas exchange was continuously analyzed (Metalyzer 3B, Cortex, Leipzig, Germany). Peak oxygen uptake ($\dot{V}O_{2\ peak}$) was defined as the highest value achieved during the test for 20s. Heart rate and a 12-lead

electrocardiogram were also continuously recorded.

Submaximal functional capacity. Functional capacity was assessed using the 6 min walk test (6MWT)[19]. The patients were instructed to cover the greatest distance possible at a self determined walking speed, in a 20 m corridor during the 6 minutes.

Quality of life. A specific scale of quality of live was assessed with Minessota Living with Heart Failure Questionnaire validated for Portuguese, during an individual interview, which measure physical and emotional dimensions[20].

Self-reported physical activity. The habitual physical activity was assessed with International Physical Activity Questionnaire (IPAQ). PA level was calculated as the sum of 7 days self report and analysed as different domains of physical activity: overall PA, leisure time PA and walking PA. When necessary, a dichotomized variable was created following the American College of Sports Medicine recommendation of > 150 minutes expended in physical activity per week[20].

Accelerometry-measured physical activity. Physical activity was objectively measured with the Tri-axial Research Tracker Accelerometer (TriTrac®, Monrovia, California, USA), with epocs of 1 minute. Patients used the accelerometer during 4 consecutive days, 2 weekdays and 2 weekend days, and the counts were converted to 7 days[22] to classify the subjects in: sedentary 0 to 99 counts; light activities 100 to 1952 counts; and moderate to vigorous activities > 1952 counts [23]. We used total counts/day, minutes spent in light and moderate-to-vigorous physical activity as direct physical activity variables.

Statistics. Statistical analysis was performed with SPSS version 18.0 (Chicago, IL, USA). Based on a previous study[19] and a handgrip weakness prevalence of 70 %, a sample size 47 patients was required for a power of 90 % and an alpha of 0.05. A *posteriori,* power calculation were performeded and results confirmed the power. Descriptive data are presented as mean ± SD. For univariate analysis, the Pearson correlation coefficient was used as a measure of association and all variables that presented $p < 0.2$ were included in the multivariable analysis. Age and gender are known to be physiological determinates of inspiratory and handgrip strength, therefore they were included in all regression models Stepwise multiple regression analysis. All data were entered as continuous variables. A two sided value of $p < 0.05$ indicated statistical significance.

Results

Fifty one patients were included in the study. Baseline characteristics of patients with CHF are given in Table 1. Patients were mostly men, overweight (47%), with predominantly hypertensive or ischemic etiology, and with systolic dysfunction. Patients were receiving guideline-recommended medications and had mild to moderate impairment in functional capacity. The prevalence of handgrip weakness was almost twofold (78 %) that of inspiratory muscle weakness (41 %). Nineteen percent of the patients had both muscle weaknesses and 16 % had no weakness.

Table 1. Baseline characteristics from heart failure patients.

Characteristics	N (%) or mean (SD)
Age (years)	58 ± 8
Gender (M/F)	43/8 (84.3/15.7)
Body mass index (kg/m^2)	28.1 ±4.3
Years of schooling	7 ± 4
Etiology of heart failure (n [%])	
Ischemic	11 (22)
Hypertensive	11 (22)
Other	29 (56)
Medications	
ACE inhibitors or ARA II	48 (94)
Diuretics	48 (94)
β blockers	48 (94)
Digoxine	31 (61)
Aldosterone Antagonist	18 (36)
Vasodilators	16 (31)
Anticoagulants	16 (31)
Antiplatelets	17 (33)
Antiarrhythmics	1 (2)
NYHA functional class (n [%])	
I	11 (22)
II	26 (51)
III	14 (27)
Left ventricular ejection fraction	
Systolic dysfunction	30 ± 8
Preserved systolic function (%)	51 ± 4 (23.5%)
Six min walk test (m)	457 ± 81
Cardiopulmonary exercise test	
VO_2 peak (ml/kg.min)	19.1 ± 5.2
V_E / VCO_2 slope	39 ± 17
RER_{peak}	1.07 ± 0.12
$HR_{\%predicted}$	85 ± 17
PI_{max} (cmH_20)	87.1± 37.6
PI_{max} (% predicted) (n [%])	82 (35.0)
Inspiratory muscle weakness (n [%])	21 (41.0)
Handgrip (N)	349 ± 102
Handgrip weakness (n [%])	40 (78.4)
Accelerometry	
Accelerometry (counts/day)	155,926 ± 64,526
Accelerometry (min of light PA)	1,295 ± 397
Accelerometry (min MV PA)	24 ± 30
Self-report Physical Activity	
IPAQ total (min)	547.6 ± 539
IPAQ leisure (min)	59 ± 99.4
IPAQ walking (min)	183.5 ± 188.1
Quality of life (score)	25.4 ± 19.0
Physical dimension score	11.8 ± 9.8
Emotional dimension score	3.8 ± 4.3

ACE – angiotensin converting enzyme; ARA – angiotensin receptor antagonist; NYHA – New York Heart Association; VO_2 – oxygen uptake; VE – minute ventilation; VCO_2 – carbon dioxide output ; PI_{max} – maximal inspiratory pressure; IPAQ – Physical Activity Questionnaire.

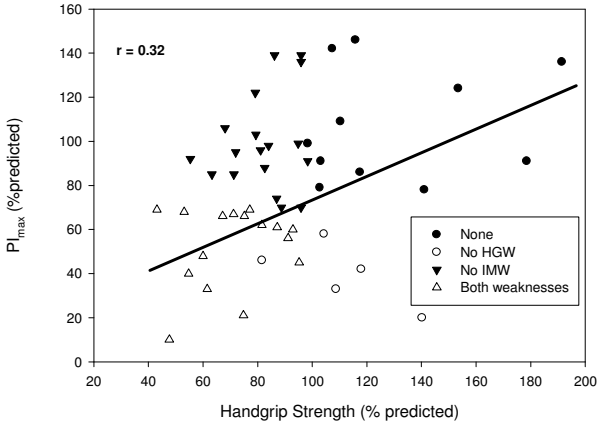

Figure 1 – Scatter plot for maximal inspiratory pressure, expressed as percentage of predicted (PI_{max} % predicted) and handgrip strength, expressed as percentage of predicted. IMW = inspiratory muscle weakness; HGW = handgrip weakness.

Table 2: Determination coefficients for candidate variables for handgrip and inspiratory muscle strength models.

Handgrip	r	p	**Maximal inspiratory pressure**	r	p
Gender	**-0.57**	**≤0.001**	**Gender**	**-0.21**	**0.14**
Age	**-0.23**	**0.11**	**Age**	**-0.08**	**0.57**
Body mass index	-0.04	0.80	Body mass index	-0.05	0.75
Schooling	**0.24**	**0.10**	**Schooling**	**0.44**	**0.001**
Medication (N)	-0.14	0.33	Medication (N)	0.16	0.27
NYHA functional class	**-0.28**	**0.045**	**NYHA functional class**	**-0.26**	**0.065**
LV ejection fraction (%)	-0.07	0.70	LV ejection fraction (%)	0.17	0.30
6 min walk test (m)	**0.41**	**0.004**	**6 min walk test (m)**	**0.42**	**0.003**
VO_2 peak (ml/kg.min)	**0.44**	**0.002**	**VO_2 peak (ml/kg.min)**	**0.21**	**0.16**
VE / VCO_2 slope	-0.05	0.74	VE / VCO_2 slope	-0.05	0.75
PI_{max}	**0.39**	**0.005**	**Handgrip**	**0.39**	**0.005**
Flexibility (cm)	**0.21**	**0.15**	**Flexibility (cm)**	**0.27**	**0.06**
Total counts	0.01	0.94	Total counts	-0.17	0.27
Moderate to vigorous PA	-0.06	0.69	Moderate to vigorous PA	-0.18	0.24
Light PA	0.07	0.63	Light PA	0.10	0.52
Total PA (IPAQ)	0.14	0.34	Total PA (IPAQ)	0.05	0.75
PA leisure time (IPAQ)	0.18	0.21	**PA leisure time (IPAQ)**	**0.20**	**0.17**
Minessota physical score	**-0.22**	**0.12**	**Minessota physical score**	**-0.24**	**0.13**
Minessota emotional score	**-0.37**	**0.008**	**Minessota emotional score**	**-0.32**	**0.02**

NYHA- New York Heart Association; LV – left ventricular; VO_2 – oxygen uptake; VE – minute ventilation; VCO_2 - carbon dioxide output; PI_{max} – maximal inspiratory pressure; PA- physical activity.

Table 2 shows the univariate analysis for candidate variables for handgrip and inspiratory strength regression models. The correlation between handgrip and inspiratory muscle strength was moderate (r=0.39, p=0.005). Figure 1 shows a scatter plot to handgrip strength and PI_{max} for age and gender predicted. Four different groups in accordance with weaknesses profile. The initial analysis showed that PI_{max} and handgrip strength were not correlated to physical activity behaviour variables, such as self-report total physical activity (IPAQ), leisure time physical activity (IPAQ), light physical activity (accelerometer), moderate-to-vigorous physical activity (accelerometer), neither to VE/VO_2 slope or left ventricular ejection fraction.

Table 3: Multivariate analysis for PI_{max} and handgrip test (stepwise regression).

Handgrip	B	P	**PI_{max}**	B	P
Gender	-0.402	0.002	Schooling	0.290	0.016
Age	-0.255	0.028	MPS	-0.354	0.004
PI_{max}	0.398	0.002	Handgrip	0.298	0.017
Model (R^2)		0.45	Model (R^2)		0.40

MPS – Minessota living with heart failure - physical score;

Table 3 shows the results of entering those significant correlates of PI_{max} and handgrip strength into a stepwise multivariable regression analysis. Age, gender, and PI_{max} were independent predictors for handgrip strength. When we analyse the same variables without patients with preserved left ventricular ejection fraction, the model was the same for handgrip strength, but not to PI_{max}. Schooling and handgrip were replaced for 6MWT, but kept the same explanation. So the model has just 2 independent predictors and both are associated with physical function (self-report – MPS; and direct measured - 6MWT). To adjust for multicollinearity, we choose the best parameter that represents physical function in each regression. From handgrip strength model we excluded 6 MWT, and from PI_{max} model we excluded VO_2 peak because both represent physical function parameters.

Discussion

In our contemporary sample of patients with CHF with systolic dysfunction as well as with preserved systolic function, handgrip strength and inspiratory muscle strength presented a moderate association ($r = 0.39$, $p = 0.005$). In accordance with previous studies[7], handgrip weakness was more prevalent than inspiratory muscle weakness in these CHF patients. However, only 19 % of our patients had both handgrip and inspiratory weakness, compatible with some level of generalized weakness. Moreover, contrary to our working hypothesis, there was no association between measures of self-reported or accelerometer measured PA with inspiratory or peripheral muscle strength. Indeed, stepwise multiple regression analysis showed that only age, gender and PI_{max} are associated with handgrip strength. On the other hand, schooling and perception of physical function scores on MLHF were the only independent predictors of PI_{max}. Altogether, these findings suggest that only a small part of inspiratory and peripheral muscle strength is determined by the variables evaluated in the present study.

Determinants of handgrip strength. The results from the stepwise analysis, which indicate that only age and gender independent predictors of handgrip strength, are in accordance with the results for healthy people[15]. Indeed, a meta-analysis about reference values for adult handgrip strength clearly demonstrates that this characteristic is gender and age specific[17]. Moreover, a recent study found a significant correlation between handgrip strength and both age and gender, respectively[24]. On the other hand, in that sample of 229

healthy individuals, they found a weaker correlation with BMI (r=0.29, p<0.0001), indicating that BMI is not the best predictor for handgrip strength, which is also in accordance with our findings[24]. Lean body mass has been related with nutritional status, handgrip strength, and lower NT-proBNP levels in heart failure patients[25].

The mechanisms underlying peripheral muscle weakness in heart failure are still controversial[26,27,28]. Peripheral weakness may be associated with very low physical activity level, which may induce atrophy. Izawa et al[29], who measured PA in CHF using pedometers, showed that VO_2 peak is closely related to PA, and that, to have 4 METs of maximal exercise capacity, patients have to perform at least 4,397 steps/day of PA. Our patients had well preserved functional capacity, with a mean VO2 peak of 5.5 METs, and, despite this, expended only a mean of 24 min per week on MV PA, indicating low levels of PA. On the other hand, Toth et al.[30] found reduced VO_{2peak} and knee extensor isometric torque in CHF when compared to healthy controls, but no difference in PA. In our sample, neither VO2 peak nor PA were correlated to handgrip strength and 18 % of patients reported to attend the recommendation to perform at least 150 min/week of PA on leisure time (IPAQ) and only 10 % attended to the recommendation for MTVPA (accelerometer measured – data not showed). When compared to the 30 % of healthy individuals who attend to this recommendation[31], this underscores the low level of PA activity of our patients. In agreement with our findings, Miller et al.[26] showed that peripheral muscle weakness of CHF patients was still prevalent, even after controlling for PA and atrophy mechanisms, suggesting that CHF patients have some intrinsic loss of strength.

Determinants of inspiratory muscle strength. PI_{max} regression showed schooling, physical score of MLHF, and handgrip strength as independent predictors. In a previous study with older individuals, respiratory muscle strength was effective to identify who are at increased risk of cardiovascular morbidity and mortality[32]. PI_{max} is also an independent predictor of mortality in heart failure patients, even in the beta-blocker era[4,33]. When we analyzed only the patients with systolic dysfunction, the results changed and self-report and objectively measured physical function point out as the main determinants to PI_{max}.

Comparing the self-reported PA and the accellerometry-measured PA, our patients seem to overestimate activities of daily life, and this may have an impact on exercise intolerance. It could be a barrier to PA, and less habitual PA drives to augmented muscle impairment or it could be a cause to symptoms (reversal causality). To explore this relationship, we performed an additional analysis using cross-tabs for physical activity and inspiratory muscle weakness. The results showed that 95% of patients that have inspiratory muscle weakness did not reach the recommendation for PA on leisure time (>150min/week; p=0.043). But even considering this, one interesting observation of the present study is that objectively measure of PA was no correlated peripheral or inspiratory

muscle strength. In agreement with our findings, some studies have shown that atrophy due to disuse cannot explain the decrease strength by itself, and cellular adaptations are more pronounced in heart failure than restricted to bed subjects[26,34].

Experimental studies have shown that the diaphragm from CHF patients presents more slow fiber type and peripheral muscle adapts with increased fast fiber types, when compared to healthy subjects[6,26,28]. But is still not clear if skeletal muscle adaptations are primary (specific myopathy), or secondary to a reduction in blood flow and abnormalities of vasomotor tone. In general, studies have shown a decreased fiber cross-sectional area, which could explain the impairment in muscle function. Despite this evidences, other studies have found preserved muscle fatigue[35], myofibrillar properties[36] and contractile protein function[37], which point out the disagreement in literature.

These evidences may support the idea that CHF patients have different mechanisms that drive them to generalized muscle weakness. A previous study from our laboratory showed that adding inspiratory muscle training to aerobic training can additionally improve outcomes like PI_{max}, VO_{2peak} and reduce VE/VO_2 slope and periodic breathing[5], suggesting that different physiological mechanisms may be involved in inspiratory and peripheral muscle training. Moreover, our multiple regression analyses showed that both models explained almost the same variance for handgrip strength (45%) and PI_{max} (40%) but the independent predictors were different. This is consistent with the literature that showed different adaptations on diaphragm muscle and skeletal muscle in this population[38,39].

Limitations. Some limitations of our study should be pointed out. One of the main limitations is the relative small sample size, so some of correlations may be underpowered and a larger sample size could have allowed subgroup analysis. We included patients with systolic dysfunction as well as with preserved systolic function to represent a wider presentation of CHF, however predictors for PI_{max} changed after diastolic dysfunction exclusion, suggesting that future studies should perform separated analyses for these patients. To evaluate peripheral and inspiratory muscle strength, we used simple volitional tests, such as handgrip and PI_{max}. Despite their known limitations as measures of muscle weakness, they are easy to use in clinical practice, they have known cut-points and also have prognostic implications. And finally, since we have a well-controlled and optimized medication sample in our outpatient clinic our results may not apply to patient with more advanced CHF. However, our sample is representative of a contemporary cohort of patients with CHF followed in a specialized clinic.

Clinical implications. Our findings may have clinical implications. The lack of association between measures of PA and muscle weakness suggests that the simple recommendation to increase PA activity may not improve muscle strength, and that formal training programs, including peripheral strength

training and inspiratory muscle training should be offered to these patients[5,40].

Conclusion

We found different correlates for peripheral and inspiratory muscle weakness in a contemporary cohort of patient with CHF due to systolic dysfunction and with preserved systolic dysfunction. Since only about 40-45 % of handgrip and inspiratory muscle strength variance can be accounted for by the variables here evaluated, future studies should be conducted to identify other determinants in this patient population.

Acknowledgements

The authors would like to acknowledgements financial support from FIPE.

Disclosure of interest

The authors declare that they have no conflicts of interest concerning this article.

Author Contributions

Conceived and designed the experiments: PABR, MSB, JPR. Data collection: MSB, PABR. Analyzed data: PABR, DBV, MSB, JPR. Wrote the paper: PABR, DBV, JPR. Final review: JPR.

References

1. Ribeiro JP; Chiappa GR; Neder, JA, Frankenstein, L. Respiratory muscle function and exercise intolerance in heart failure. Curr Heart Fail Rep. 6(2):95-101, 2009.
2. Wong E, Selig S, Hare DL. Respiratory muscle dysfunction and training in chronic heart failure. Heart, Lung and Circulation 20:289-294, 2011.
3. Savage PA, Shaw AO, Miller MS, VanBuren P, LeWinter MM, Ades PA, Toth MJ. Effect of resistance training on physical disability in chronic heart failure. Med Sci Sports Exerc. 43(8):1379-86, 2011.
4. Meyer FJ, Borst MM, Zugck C, Kirschke A, Schellberg D, Kübler W, Haass M. Respiratory Muscle Dysfunction in Congestive Heart Failure. Circulation 103:2153-2158, 2001.
5. Winkelmann E, Chiappa GR, Lima COC, Viecili PRN, Stein R, Ribeiro JP. Addition of Inspiratory Muscle Training to Aerobic Training Improves Cardiorespiratory Responses to Exercise in Patients with Heart Failure and Inspiratory Muscle Weakness. The American Heart Journal, v. 158, p. 768.e1-768.e7, 2009.
6. Georgiadou P, Adamopoulos S. Skeletal muscle abnormalities in chronic heart failure. Curr Heart Fail Rep, 9:128-132, 2012.
7. Chua TP, Anker SD, Harrington D, Coats AJ. Inspiratory muscle strength is a determinant of maximum oxygen consumption in chronic heart failure. Br Heart J. 74(4):381-5, 1995.
8. Hammond MD, Bauer KA, Sharp JT, Rocha RD. Respiratory muscle strength in congestive heart failure. Chest. 98(5):1091-4, 1990.
9. Mezzani A, Corrà U, Baroffio C, Bosimini E, Giannuzzi P. Habitual activities and peak aerobic capacity in patients with asymptomatic and symptomatic left ventricular dysfunction. Chest. 117(5):1291-9, 2000.
10. Carmeli E, Coleman R, Reznick AZ. The biochemestry of age muscle. Experimental Gerontology 37 :477-489, 2002.
11. Short KR, Vittone JL, Bigelow ML, Proctor DN, Coenen-Schimke JM, Rys P, Nair KS. Changes in myosin heavy chain mRNA and protein expression in human skeletal muscle with age and endurance exercise training. J Appl Physiol. Jul;99(1):95-102, 2005.
12. Toth MJ, Miller MS, VanBuren P, Bedrin NG, LeWinter MM, Ades PA, Palmer BM. Resistance training alters skeletal muscle structure and function in human heart failure: effects at the tissue, cellular and molecular levels. J Physiol. 590(Pt 5):1243-59, 2012.
13. Swedberg et al. Guidelines for the diagnosis and treatment of chronic heart failure: executive summary (update 2005). The Task Force for the Diagnosis and Treatment of Chronic Heart Failure of the European Society of Cardiology. Eur Heart J 26:115-40, 2005.
14. Chiappa GR, Roseguini BT, Vieira PJ, Alves CN, et al. Inspiratory muscle training improves distribution of blood flow to resting and exercising limbs in patients with chronic heart failure. J Am Coll Cardiol. 51(17):1663-71, 2008.
15. Neder JÁ, Andreoni A, Lerario MC, Nery LF. References values for lung function tests. II Maximal respiratory pressures and voluntary ventilation. Brazilian Journal of Medical and Biological Research Brazilian Journal of Medical and Biological Research, 32:719-27, 1999.
16. Izawa KP, Watanabe S, Osadab N, Kasaharaa Y, Yokoyamaa H, Hirakia K, Morioa Y, Yoshiokaa S, Okac K, Omiyab K. Handgrip strength as a predictor of prognosis in Japanese patients with congestive heart failure. European Journal of Cardiovascular Prevention and Rehabilitation 16:21–27, 2009.
17. Bohannon RW, Peolsson A, Massy-Westropp N, Desrosiers J, Bear-Lehman J. Reference values for adult grip strenght measured with a Jamar dynamometer : a descripted meta-analysis. Physioterapy 92 :11-15, 2006.
18. Dall'Ago P, Chiappa GR, Guths H, Stein R, Ribeiro JP. Inspiratory muscle training in patients with heart failure and inspiratory muscle weakness: a randomized trial. J Am Coll Cardiol. 47: 757-63, 2006.
19. Witham M, Argo I, Johnston D, Struthers AD, McMurdo MET. Predictors of exercise capacity and everyday activity in older heart failure patients. The European Journal of Heart Failure 8: 203 – 207, 2006.
20. Carvalho VO, Guimarães GV, Carrara D, Bacal F, Bocchi EA.Validation of the Portuguese version of the Minnesota Living with Heart Failure Questionnaire. Arq Bras Cardiol. 93(1):39-44, 2009.

21. Blissmer B, Deschenes MR, Franklin BA, Lamonte MJ, Lee IM, Nieman DC, Swain DP; American College of Sports Medicine. American College of Sports Medicine position stand. Quantity and quality of exercise for developing and maintaining cardiorespiratory, musculoskeletal, and neuromotor fitness in apparently healthy adults: guidance for prescribing exercise. Med Sci Sports Exerc.43(7):1334-59, 2011.
22. Reichert FF, Menezes AM, Kingdom Wells JC, Ekelund E, Rodrigues FM, Hallal PC. A methodological model for collecting high-quality data on physical activity in developing settings-the experience of the 1993 Pelotas (Brazil) Birth Cohort study. J Phys Act Health. 6(3):360-6, 2009.
23. Freedson PS, Melanson E, Sirard J. Calibration of the Computer Science and Applications, Inc. accelerometer. Med Sci Sports Exerc. 30(5):777-81, 1998.
24. Chandrasekaran B, Ghosh A, Prasad C, Krishnan K, Chandrasharma B. Age and anthropometric traits predict handgrip strength in healthy normals. J Hand Microsurg. 2(2):58-61, 2010.
25. Oreopoulos A, Ezekowitz JA, McAlister FA, Kalantar-Zadeh K, Fonarow GC, Norris CM, Johnson JA, Padwal RS. Association between direct measures of body composition and prognostic factors in chronic heart failure. Mayo Clin Proc. 85(7):609-17, 2010.
26. Miller MS, Vanburen P, Lewinter MM, Lecker SH, Selby DE, Palmer BM, Maughan DW, Ades PA, Toth MJ. Mechanisms underlying skeletal muscle weakness in human heart failure: alterations in single fiber myosin protein content and function. Circ Heart Fail. 2(6):700-6, 2009.
27. van Hees HWH, van der Heijden HFM, Ottenheijm CAC, Heunks LMA, Pigmans CJC, Verheugt FWA, Brouwer RMHJ, Dekhuijzen PNR. Diaphragm single-fiber weakness and loss of myosin in congestive heart failure rats. Am J Physiol Heart Circ Physiol, 293, pp H819-H828, 2007.
28. Nicoletti I, Cicoira M, Zanolla L, Franceschini L, Brighetti G, Pilati M, Zardini P. Skeletal muscle abnormalities in chronic heart failure patients: relation to exercise capacity and therapeutic implications. Congest Heart Fail. 9(3):148-54, 2003.
29. Izawa KP, Watanabe S, Oka K, Hiraki K, Morio Y, Kasahara Y, Takeichi N, Tsukamoto T, Osada N, Omiya K. Physical activity in relation to exercise capacity in chronic heart failure patients. Int J Cardiol. 152(1):152-3, 2011.
30. Toth MJ, Shaw AO, Miller MS, VanBuren P, LeWinter MM, Maughan DW, Ades PA. Reduced knee extensor function in heart failure is not explained by inactivity. Int J Cardiol. 143(3):276-82, 2010.
31. Rombaldi AJ, Menezes AM, Azevedo MR, Hallal PC. Leisure-time physical activity: association with activity levels in other domains. J Phys Act Health. 2010 Jul;7(4):460-4.
32. van der Palen J, Rea TD, Manolio TA, Lumley T, Newman AB, Tracy RP, Enright PL, Psaty BM. Respiratory muscle strength and the risk of incident cardiovascular events. Thorax. 59(12):1063-7, 2004.
33. Frankenstein L, Nelles M, Meyer J, Sigg C, Schellberg D, Remppis A, Katus HA, Zugck C. Validity, prognostic value and optimal cutoff of respiratory muscle strength in patiens with chronic heart failure changes with beta-blocker treatment. Eur J Cardiovasc Prev Rehabil 16:424-429, 2009.
34. Vescovo G, Serafini F, Facchin L, Tenderini P, Carraro U, Dalla Libera L, Catani C, Ambrosio GB. Specific changes in skeletal muscle myosin heavy chain composition in cardiac failure: differences compared with disuse atrophy as assessed on microbiopsies by high resolution electrophoresis. Heart 76(4): 337-43, 1996.
35. Munkvik M, Lunde PK, Aronsen JA, Birkeland JAK, Sjaastad I, Sejersted OL. Attenuated fatigue in slow twich skeletal muscle during isotonic exercise in rats with chronic heart failure. PLoS one, v. 6 (7), 2011.
36. De Sousa E, Veksler V, Bigard X, Mateo P, Ventura-Clapier R. Heart failure affects mitochondrial but not myofibrillar intrinsic properties of skeletal muscle. Circulation. 10;102(15):1847-53, 2000.
37. Okada Y, Toth MJ, VanBuren P. Skeletal muscle contractile protein function is preserved in human heart failure. J Appl Physiol 104:952-957, 2008.
38. Stassijns G, Lysens R, Decramer M. Peripheral and respiratory muscles in chronic heart failure. Eur Respir J. 9(10):2161-7, 1996.
39. Drexler H, Riede U, Munzel T, Konig H, Funke E, Just H. Alterations of skeletal muscle in chronic heart failure. Circulation 85: 1751-1759, 1992.
40. Laoutaris ID, Adamopoulos S, Manginas A, Panagiotakos DB, Kallistratos MS, Doulaptsis C, Kouloubinis A, Voudris V, Pavlides G, Cokkinos DV, Dritsas A. Benefits of combined aerobic/resistance/inspiratory training in patients with chronic heart failure. A complete exercise model? A prospective randomised study. Int J Cardiol. 2012 [Epub ahead of print]

ARTIGO II

Contractile properties of myocardium myofibrils isolated from mice with heart-specific deletion of arginyl-tRNA-protein transferase

Propriedades contráteis de miofibrilas isoladas de miocárdio de camundongos com knockout cardíaco específico para arginil-transferase

Contractile properties of myocardium myofibrils isolated from mice with heart-specific deletion of arginyl-tRNA-protein transferase

Paula A.B. Ribeiro [1], Jorge P. Ribeiro[1], Fabio Minozzo[2], Ivan Pavlov [2], Nicolae Adrian Leu [3], SatoshiKurosaka[3], Anna Kashina[3], Dilson E. Rassier[2 4]

[1]Exercise Pathophysiology Research Laboratory and Cardiology Division, Hospital de Clínicas de Porto Alegre ; Faculty of Medicine, Federal Universityh of Rio Grande do Sul, Porto Alegre, Brazil;
[2] Department of Kinesiology, McGill University, Canada.
[3]Department of Animal Biology, School of Veterinary Medicine, University of Pennsylvania, USA
[4] Departments of Physics and Physiology, McGill University, Canada.

Abstract

Protein arginylation is a cellular process catalyzed by arginyl-tRNA-protein transferase (Ate1). Mice with the α-MHC Ate1 knockout (Ate1 CKO) present late life lethality as well as defects in cardiovascular development, including myofibril disorganization, which developcongestive heart failure. In this study, we compared passive forces and contractile properties, at sarcomere lengths (SL) between 1.8 and 2.6µm, of myofibrils isolated from the myocardium muscle from Ate1 CKO with those from wild-type (WT) mice. The maximal isometric forces were lower in Ate1 CKO myofibrils (102.2 ± 11.0 nN/µm2) than in WT myofibrils (151.3 ± 11.7 nN/µm^2), which was accompanied by a downwards shift in the passive force-SL curve, suggesting that Ate1 CKO myofibrils are weaker and less stiff. The rate of force development (K_{act}) was similar between groups (Ate1 CKO: 3.1 ± 0.4 sec^{-1}, WT: 3.3 ± 0.5 sec^{-1}). The rate of force redevelopment (K_{tr}) following a shortening-stretch protocol was also similar between groups (Ate1 CKO: 4.7 ± 2.2 sec^{-1}, WT: 6.6 ± 0.8 sec^{-1}), which suggests that changes in force are not associated with cross-bridge kinetics and thin filament activation. The rates of relaxation upon muscle deactivation (K_{rel}) was similar among groups at most SL investigated, although there was a tendency for Ate1 CKO myofibrils to become slower when measurements were made at short SL. Overall, these results demonstrate that arginylation affects contractile proteins and passive structures within sarcomeres, suggesting that it is an important mechanism associated with force regulation in cardiac myofibrils.

Key words: Ate1 CKO, sarcomere, myosin, titin, heart, cardiomyopathy

Introduction

Protein arginylation is a post-translational cellular process catalyzed by arginyl-tRNA-protein transferase (Ate1)[1], responsible for transferring arginine (Arg) from tRNA into proteins[2,3,4]. Argilynation is important for many aspects of cell and cardiovascular development[5]. Ate1 knockout mice (Ate1 CKO) have been successfully developed in recent years, resulting in high embryonic lethality and severe defects in cardiovascular development and angiogenesis[6]. Recently, we developed a mouse with deletion of Ate1 in differentiated cardiac myocytes with alpha myosin heavy chain promoter (α-MHC Ate 1 CKO mouse) that induces dilated cardiomyopathy and leading to late postnatal lethality, with characteristics that are reminiscent of age-related heart failure in humans[7]. Therefore, the specific involvement of cardiomyocites in these animals may result in an appropriate model to investigate cardiomyopathy and heart failure.

While most studies investigating cardiac muscle mechanics have been conducted with whole muscle[8], myocytes or muscle strips from the heart[9,10], these preparations contain complex extracellular structures, and thousands of sarcomeres arranged in series and in parallel, making

interpretation of contractile properties at the molecular level limited. Furthermore, the formation of activation gradients in cardiomyocytes due to Ca^{2+} diffusion may provide confounding results[11]. We have overcome these limitations by using isolated cardiac myofibrils, which have a small diameter (<2 μm) and therefore short diffusion distance for activation of the contractile apparatus. We have used a newly developed system with the capability to measure forces with a high signal-noise ratio[12] together with a perfusion switching technique[13,14] that allows fast solution exchange in the experimental milieu, while measuring real-time images of sarcomeres during the experiments. We havepreviously investigated the active and passive force development in α-MHC Ate 1 CKO mousein different sarcomere lengths, which allowed us to construct a force-sarcomere length relation for these preparations – the cellular basis of the Frank-Starling law of the heart[15]. Analysis of cardiac myocytes isolated from α-MHC Ate 1 CKO mouserevealed a general impairment in myofibril active and passive strength, heart integrity, myofibril development, and disorganization, including sarcomere collapse and disintegration of the intercalated disks among myofibrils, findings that worsen with age[17].

Anticipating that α-MHC Ate 1 CKO mousewould present smaller levels of active force, we aimed to understand the molecular mechanisms of myofibrils weakness. A smaller active force production could solely result from fewer myosin cross-bridges attached to actin during activation, due to disorganization of sarcomeres, but it could also affect the rate constants of myosin cross-bridges shifting from weakly bound to strongly bound states. Thus, in the present report, using new experiments, we extend our previous observations[10] to evaluated the rates of force development (K_{act}), redevelopment (K_{tr}) following a shortening-stretch protocol, and relaxation (K_{rel}) during and after activation, parameters that provide information on myosin cross bridges kinetics.

Methods

Generation of αMHC-*Ate1* mice. A mouse model with cardiomyocyte specific Ate1 CKO was created using a previously developed '*Ate1*-floxed' mouse line[16,17], which was crossed with αMHC-Cre mice[18], in which Cre-recombinase is expressed under cardiomyocyte-specific α-myosin heavy chain promoter, that activates upon differentiation, resulting in Ate1 deletion in the heart muscle (α MHC Ate 1 CKO mice). To confirm the effectiveness and specificity of the Cre-transgene expression, we crossed αMHC-Cre mice to the R26R Rosa reporter mouse strain, in which LacZ expression occurs following Cre-mediated excision of a repressor element and thus is confined specifically to the Cre-expressing tissues. X-gal staining of α-MHC-Cre embryos at E10.5 showed specific Cre expression in the embryonic heart. Details of generation of the α-MHC Ate 1 CKO mice have been previously presented[10] (Anexo2).

Animals. Six female mice with heart-specific deletion of arginyl-tRNA-protein transferase (α-MHC Ate 1 CKO mice) and 6 age- and gender-matched wild type mice (WT) were used in this study. The animals were >1 year old (mean= 461±40 days). Mice were euthanized and dissected to assess the chest cavity for hearts extraction.

Electron microscopy. Muscle samples of the hearts were prepared for electron microscopy according to standard procedures in our laboratory[19]. Briefly, hearts were washed in PBS and fixed in 2.5% glutaraldehyde and 2% paraformaldehyde in a buffer containing 0.1 M sodium cacodylate (pH 7.4) at 4°C, followed by two washes and post-fixation in 2% osmium tetroxide. For staining, fixed hearts were washed twice for 10 minutes each in the same buffer, once for 10

minutes in distilled water, incubated 1 hour at room temperature in a 2% aqueous solution of uranyl acetate. Stained hearts were then dehydrated by incubation for 10 minutes in 50%, 70%, 80%, 90% and 100% ethanol, followed by two 5-minute incubations in propylene oxide (PO), overnight incubation in 1:1 PO:Epon (Poly/Bed 812, Polysciences), and then 1 day in 100% Epon. Epon-embedded hearts were kept for 2 days at 60°C for Epon polymerization, after which they were sectioned, stained with 1% uranyl acetate in 50% methanol and with a 2% (w/v) solution of bismuth subnitrite at 1:50 dilution. Finally, the hearts were overlaid onto Formvar-coated grids for electron microscopy.

Experiment preparations for analysis of mechanical properties of the heart. Small sections of myocardium were extracted from WT and CKO hearts and were tied to wood sticks, gently cleaned in rigor solution (50mM Tris pH 7.0, 100 mMNaCl, 2 mMKCl, 2 mM $MgCl_2$, and 10 mM EGTA), and stored in rigor/glycerol solution (1:1 v/v) at -20°C. On the day of experiments, small pieces of the sample were homogenized in rigor solution (homogenizer VWR AHS250, Canada) following standard procedures[20] which resulted in a solution containing small bundles of myofibrils. The myofibrils were transferred to an experimental chamber, which was kept at a constant temperature of 10°C during the experiments. Small bundles of 3-12 myofibrils were chosen for mechanical testing based on striation pattern and number of sarcomeres in series (between 10 and 30). The myofibrils were glued between an atomic force cantilever (AFC, model ATEC-CONTPt, Nanosensors, USA; mean stiffness = 0.2 N/m) and a stiff glass microneedle (stiffness >2000nN•μm^{-1}) and lifted off the glass slide by ~1µm using micromanipulators (Narishige NT-88-V3, Japan). The stiff microneedle was connected to a motor arm, allowing for computer-controlled length changes in the myofibrils during the experiments. The attached myofibril was centered in the microscope optical field under low magnification (10X-20X). Imaging of the myofibrils was achieved with a CCD camera (Go-3, QImaging, USA; pixel size: 3.2µm X 3.2µm; final resolution 0.035µm) under high magnification provided by a phase contrast lens (Nikon plan-fluor, 60X, NA 0.70), and increased 1.5X by an internal microscope function. The contrast between the dark bands of myosin (A-bands) and the light bands of actin (I-bands) provided a dark-light intensity pattern representing the striation pattern produced by the sarcomeres, which allowed precise measurements of sarcomere length during the experiments.

Myofibrils were activated/ deactivated by quickly changing the solution surrounding the myofibrils (relaxing, pCa^{2+} 9.0 and activating, pCa^{2+} 4.5) using a multi-channel perfusion system (VC–6M, Harvard Apparatus, USA) attached to a double-barreled pipette, as previously described[12]. The pipette was placed close to the myofibrils (~100µm), and the solutions were continuously dragged from the chamber through a back channel by using a peristaltic pump (Instech P720, Harvard Apparatus, USA); the flow rate achieved with this system was ~5µl•sec^{-1}. When surrounded by the activating solution (pCa^{2+} 4.5), the myofibrils contracted and produced force, which caused deflection of the AFC. The deflection was detected and recorded using an optical system that allows for high time-resolution measurements of mechanical properties of myofibrils[12]. Since the stiffness of the AFC (K) is known and the amount of cantilever displacement produced by the contraction (Δd) is tracked during the experiments, the force (F) could be calculated as $F = K \bullet \Delta d$.

Measurements of active and passive myofibril forces. Once myofibrils were attached to the AFC and micro-needles, they were passively adjusted to average sarcomere lengths of 1.8 µm, 2.0 µm, 2.2µm, 2.4µm or 2.6µm (random order) before activation to test the length dependence of active force production. The solution surrounding the myofibrils was exchanged from pCa^{2+} 9.0 to pCa^{2+} 4.5, which caused activation and force development. Once the myofibrils were fully activated and maximal force was obtained, the myofibrils underwent a shortening-stretching protocol (amplitude 30% SL; 360µ/sec); interval between length changes: 5ms) during which the force declined and rapidly re-- developed to attain a new steady-state level. Myofibrils were excluded if the control isometric force decreased by ≥20% of maximal force production during the course of the experiments. After myofibrils were tested in all SL, the myofibrils were tested for passive forces. The myofibrils were stretched passively (pCa^{2+} 9.0) in consecutive steps of 0.2µm/sarcomere at a speed of 10µm/sec, starting from a SL of 1.8µm up to a SL of 2.6µm.

Data analysis. The maximal force produced by the myofibrils was calculated after the initial force development stabilization and after force redevelopment following the shortening-stretch protocol. Forces were averaged for a period of 2 sec to avoid potential artifacts interfering with measured values. The passive forces produced by myofibrils during the step protocol were calculated after the stretches, when the force was stabilized in every SL. All forces were normalized by the myofibril cross sectional area (CSA) and number of the myofibrils, assuming circular geometry.

For each contraction, we analyzed the rate of force development (K_{act}), the rate of redevelopment (K_{tr}) after the shortening-stretch protocol, and the rate of exponential relaxation following myofibril deactivation (K_{rel}). For determination of K_{act} and K_{tr} we fitted the force curve with a two-exponential equation (a*(1-exp(-k*t)-exp(-l*t))+b). For determination of K_{rel} we fitted the data with a single-exponential equation (a*exp(-k*(t-c))+b). For both equations, *F* is force, *t* is time, K_1 and K_2 are rate constants for force development, *a* is the amplitude of the exponential(s), and *b* is the initial force value.

Statistics. The variables with normal distribution were presented as mean ± standard error. Those variables without normal distribution were expressed as geometric mean and confidence intervals and transformed to Log_{10}. The comparisons between two groups were performed using ANOVA-two way for repeated measures. Multiple comparisons were performed using the Bonferroni correction. A $p \leq 0.05$ was accepted for all comparisons.

Results

Figure 1 shows electron microscopy pictures taken from heart muscles dissected from WT and CKO mice. There were visible defects in myofibril formation in the CKO mice: significant miss-alignments between myofibrils and large sarcomere pattern disorganization are seen in these pictures. In the CKO hearts, some of sarcomeres are split, and there is extra space between parallel myofibrils, not seen in WT hearts. Most importantly, the A-band and the M-lines are not clearly defined, suggesting that there is significant displacement of some of the thick filaments from the center of sarcomere. Although titin filaments are not visible in this picture, displacements of thick filaments form the center of the sarcomere are common when titin is dislodged from Z-lines, or when titin has weakened due to an increased compliance.

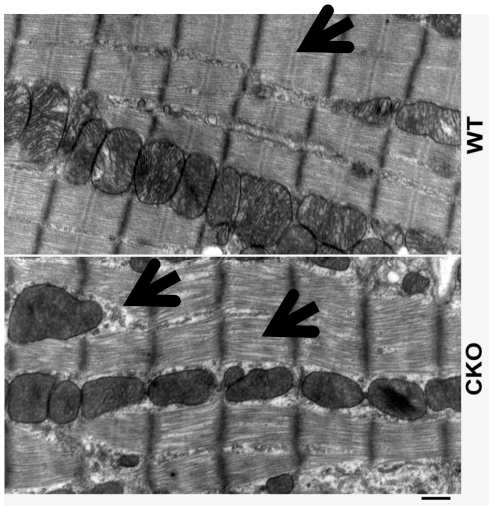

Figure 1 - electron microscopy pictures taken from heart muscles dissected from wild type (WT) and knockout mice (CKO). The arrows indicate A-band and the M-lines in WT but not in CKO, and an example of split and misalignment area.

Active and passive forces. Figure 2A shows a representative example of fittings for force trace curves obtained with myofibrils isolated from WT and Ate1 CKO muscles and contractions produced during a typical experiment. During activation of the myofibrils, force increased rapidly and reached a steady-state level. Note that the force traces present a very clear pattern and high signal : noise ratio, which allows us to compare small changes in force development, not always possible with cardiomyocite experiments. In this example, the force produced by the Ate1 CKO myofibril was 48% smaller than the force produced by the WT myofibril, a pattern that was consistent across experiments. This difference was confirmed statistically when all forces are compared in the two groups (irrespective of sarcomere length). The WT myofibrils produced 132 ± 10.8 nN/μm^2 while the Ate1 CKO myofibrils produced 89.1±9.04 nN/μm^2 of force during full activation.

The decrease in force that was observed in Ate1 CKO myofibrils was not influenced by sarcomere length ($p=0.057$) – the force was smaller in Ate 1 CKO myofibrils in all lengths investigated ($p<0.001$). Figure 2B shows contractions produced by different myofibrils than those depicted in Figure 2A, in sarcomere lengths of 2.2μm and 2.4μm. Ate1 CKO myofibrils presented reduction in force in both cases. Note that increasing in the initial sarcomere length previous to activating the myofibrils lead to an increase in the passive forces in both myofibrils, albeit by different magnitudes – the passive force was smaller in Ate1 CKO myofibrils. These results were confirmed statistically for all myofibrils investigated in this study at increasing sarcomere length (Figure 3A).

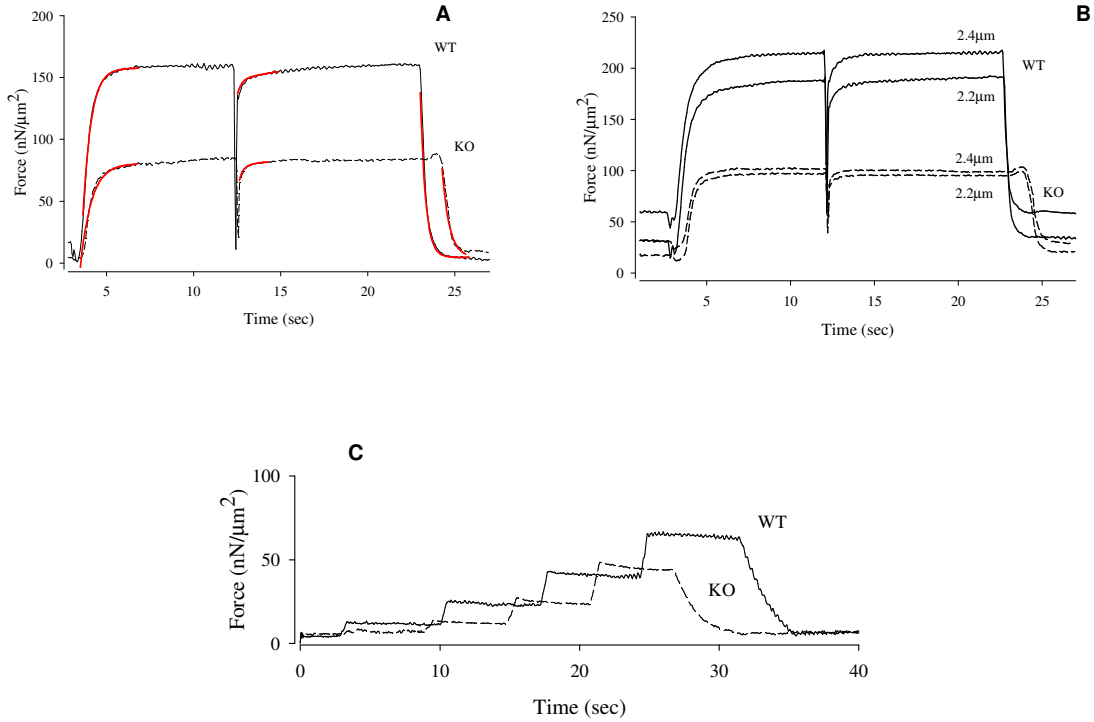

Figure 2- Panel A - typical data for CKO and WT maximal contraction. Red lines represent the kinetic adjustments for force development (Kact), force redevelopment (Ktr) and relaxation (Krel). **Panel B –** two different sarcomere length (2.2 and 2.4) for WT and CKO (dotted trace) mice representing the force-length relationship. **Panel C -** Step protocol induced to consecutive passive stretches (pCa^{2+} 9.0) in different SL for Ate1 α-MHC mouse (CKO) dotted trace, and wild type (WT) continuous trace.

Figure 2C shows a representative example of the step protocol induced to the As expected, each stretch imposed to the myofibrils lead to an increase in passive force[21,22]. Myofibrils isolated from Ate1 CKO muscles produced smaller increases in passive forces during the stretch protocol ($p=0.007$), a result that was confirmed in all experiments (Figure 3B) ($p<0.001$ for SL), and but not showed a interaction effect, suggesting that Ate1 CKO myofibrils are more compliant than WT myofibrils.

Rates of development, redevelopment, and relaxation. After maximal activation was obtained, the myofibrils were rapidly shortened and re-stretched back to the initial length, a common protocol used for the investigation of force redevelopment under full activation[23,24]. In Figures 2A and myofibrils at the end of the experiment, i.e. consecutive passive stretches (pCa^{2+} 9.0). 2B, it is clear that force decreases significantly as result of the shortening-stretching protocol, and immediately after it re-develops to attain a new steady-state force level that is similar to the level it was before the imposed length changes. The fast decrease in force during shortening is assumedly associated with a forcibly breakage of myosin-actin interactions, after which myosin cross-bridges will re-attach to actin and redevelop force (as depicted in Figure 2A). When the myofibrils are surrounded by the relaxing solution (pCa^{2+} 9.0), they rapidly relax.

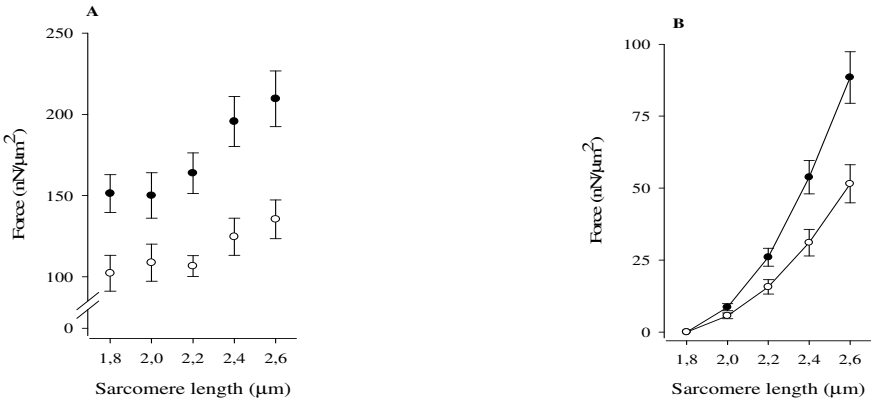

Figure 3 – Panel A: Absolut active force per CSA in different SL. There was difference between groups ($p<0.001$) but not SL.Panel B: Passive force per CSA in different SL, difference between groups ($p=0.007$) and SL ($p<0.001$).

The values for K_{act} and K_{rel} were influenced by sarcomere length ($p <0.01$ and $p=0.043$, respectively) (Figures 4A, 4C). The K_{tr} following a shortening-stretch protocol was also similar between groups and not influenced by SL, and when analyzed all together were similar (Ate1 CKO: 4.7 ± 2.2 sec^{-1}, WT: 6.6 ± 0.8 sec^{-1})(Figure 4B). These results suggest that, while Ate1 CKO myofibrils are weaker than WT myofibrils, such decrease in force is not associated with cross-bridge kinetics and thin filament activation.

Discussion

The main findings of this study were that: (i) myofibrils isolated from Ate 1CKO mice presented a decreased active and passive force in several sarcomere lengths; and that (ii) this decrease in active force was not followed by changes in the rate of force development (K_{act}) and redevelopment (K_{tr}) after a shortening-stretch protocol. The rate of relaxation (K_{rel}) was not changed in the Ate 1 CKO myofibrils either; although there was a tendency for a slower relaxation in shorter SL. Altogether, these findings suggest that the cardiac Ate 1 CKO myofibrils force impairment does not affect cross-bridge kinetics.

In previous studies using a complete *Ate1* mouse CKO – instead of a conditional deletion as done in the current study - it was observed that arginylation is essential for cardiac morphogenesis and embryogenesis[6,19].

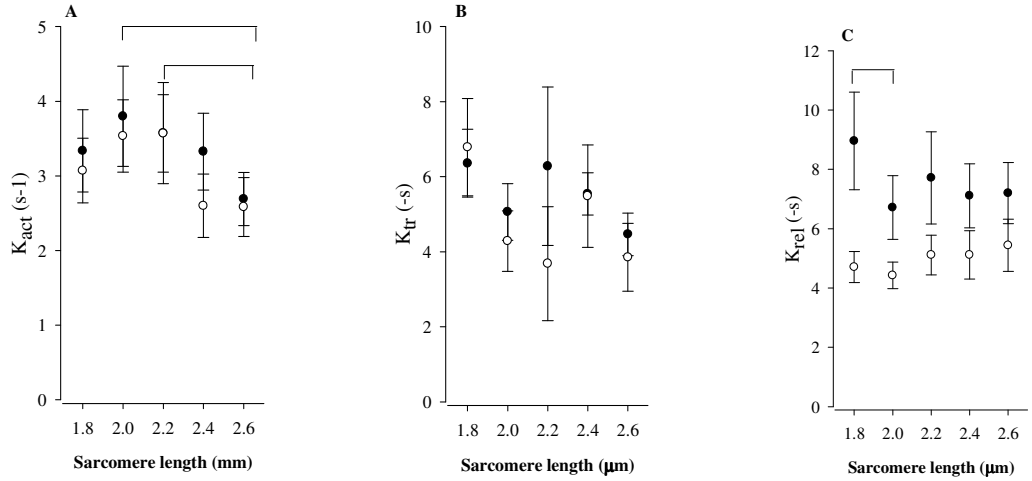

Figure 4 - Panel A: Kinetic for force development (K_{act}) in different SL. There was difference between 2.0 µm and 2.2 µm to 2.6 µm. Panel B: Kinetic for force redevelopment (K_{tr}) in different SL. Panel C: Kinetic for relaxation (K_{rel}) in different SL. The difference is between 1.8µm and 2.0 µm.

These studies suggested that several properties of the heart were affected by lack of argynilation, but the deletion of Ate1 was not specific to the heart. Subsequently, we used a highly specific, conditional deletion of *Ate1* in the heart in which *Ate1* deletion was driven by α-myosin heavy chain promoter (Ate 1 CKO mice)[10]. The lack of argynilation in these hearts affected important proteins, including myosin heavy chains, titin N2B, tropomyosin-α 1 and cardiac troponin T2 [10]. The CKO mice had higher mortality when compared to WT at 3 months, and their hearts were enlarged at 12 months. Cardiac contractility defects and dilated cardiomyopathy were observed, accompanied by defects in cardiac myofibril organization. Figure 1 shows that the hearts used in the current study also showed defects accompanied by large structural abnormalities in myofibrils. The myofibrils were disorganized, and filaments seem to be randomly oriented in several sections of the sarcomeres.

Of special interest in our previous study was the fact that many myofibril proteins were arginylated on specific sites, including MHC and titin[10]. These proteins have well defined roles in establishing contractility, and sarcomeric structure and integrity. They are intrinsically associated with active and passive force generation. Consistently, in the present study, we observed that myofibrils isolated from α Ate 1 CKO1 mouse produced less active and passive force than WT in a range of sarcomere lengths covering the entire force-length relation for cardiac muscle (Figure 3), which lead us to investigate further the causes of force deficit. The lower active force production observed in our study could be a consequence of alterations in sarcomere structure and organization of filaments, resulting either in fewer myosin cross-bridges attached to actin during activation due to structural disorganization or slower transitions from "weak to strong-binding" cross-bridge molecular states. This could also be reflected in changes in the rate constants of force development (K_{act}), re-development (K_{tr}) and relaxation (K_{rel}). Since K_{act} and K_{tr} were clearly not affected in the myofibrils isolated from the Ate1 CKO mice, our results suggest that most of the changes we observed in active and passive forces are associated with disorganization of the sarcomeres. Therefore, cross-bridge kinetics could possibly not be so affected.

Changes in passive forces are likely associated with changes in titin content and/or its isoforms, as it has been observed in different heart diseases[30,22,25]. Interestingly, titin becomes stiffer with some conditions that affect the muscular system, as in spasticity[26] or hypertension[27], but it becomes more compliant in others, such as in dilated cardiomyopathy[9], chronic pulmonary disease[28], and mechanically ventilated diaphragms[29]. In the case of the myofibrils from the Ate 1 CKO mice, the myofibrils were more compliant than in WT, as shown by a downward shift in the passive force-sarcomere length relationship (Figure 3B). These changes in may improve diastolic filling by lowering overall myocardial stiffness[30,31], and thus they may have a significant impact in the heart. Indeed, the findings of reduced myofibril stiffness in our model are consistent with the results of Nagueh et al[30], who evaluated muscle strips from patients with dilated cadiomyopathy and found improved diastolic function.

Overall, our results confirm our previous findings that arginylation affects contractile proteins and passive structures within sarcomeres, suggesting that it is an important mechanism associated with force regulation in cardiac myofibrils[31]. These abnormalities were not accompanied by changes in the rate of force development (K_{act}) and redevelopment (K_{tr}) after a shortening-stretch protocol, suggesting that the cardiac Ate 1 CKO myofibrils force impairment does not affect cross-bridge

kinetics. Moreover, our findings are in agreement with previous studies in human dilated cardiomyopathy[30], suggesting that α-MHC Ate1 knockout mouse may be a reliable animal model for the study of CHF.

References

1. Balzi E, Choder M, Chen WN, Varshavsky A and Goffeau A. Cloning and functional analysis of the arginyl-tRNA-protein transferase gene ATE1 of Saccharomyces cerevisiae. J Biol Chem 265: 7464-7471, 1990.
2. Kaji A, Kaji H and Novelli G D. A soluble amino acid incorporating system. Biochem Biophys Res Commun. 10: 406-409, 1963.
3. Soffer RL. The arginine transfer reaction. Biochim Biophys Acta 155: 228-240, 1968.
4. Takao K, and Samejima K. Arginyl-tRNA-protein transferase activities in crude supernatants of rat tissues. Biol Pharm Bull 22: 1007-1009, 1999.
5. Lamon KD, Kaji H. Arginyl-tRNAtransferase activity as a marker of cellular aging in peripheral rat tissues. ExpGerontol. 15(1):53-64, 1980.
6. Kwon YT, Kashina AS, Davydov IV, Hu RG, An JY, Seo JW, Du F, Varshavsky A. An essential role of N-terminal arginylation in cardiovascular development. Science 297: 96-99, 2002.
7. Kurosaka S, Leu NA, Pavlov I, Han X, Ribeiro PA, Xu T, Bunte R, Saha S, Wang J, Cornachione A, Mai W, Yates JR 3rd, Rassier DE, Kashina A. Arginylation regulates myofibrils to maintain heart function and prevent dilated cardiomyopathy. J Mol Cell Cardiol. 2012 May 21. [Epub ahead of print]
8. MacFarlane NG, Darnley M, Smith GL. Cellular basis for contractile dysfunction in the diaphragm from a rabbit infarct model of heart failure. Am J Physiol Cell Physiol 278:C739-C746, 2000.
9. Nagueh SF, Shah G, Wu Y, Torre-Amione G, King NM, Lahmers S, Witt CC, Becker K, Labeit S and Granzier HL. Altered titin expression, myocardial stiffness, and left ventricular function in patients with dilated cardiomyopathy. *Circulation* 110: 155-162, 2004.
10. Kreutziger KL, Piroddi N, McMichael JT, Tesi C, Poggesi C, RegnierM.Calcium binding kinetics of troponin C strongly modulate cooperative activation and tension kinetics in cardiac muscle. J Mol Cell Cardiol 50:165-174, 2011.
11. terKeurs HE, Shinozaki T, Zhang YM, Zhang ML, Wakayama Y, Sugai Y, Kagaya Y, Miura M, Boyden PA, Stuyvers BD, Landesberg A. Sarcomere mechanics in uniform and non-uniform cardiac muscle: a link between pump function and arrhythmias. Prog Biophys Mol Biol. 97:312-31, 2008.
12. Labuda A, Brastaviceanu T, Pavlov I, Paul W and Rassier DE. Optical detection system for probing cantilever deflections parallel to a sample surface. Rev Sci Instrum 82, 013701, 2011.
13. Stehle R, Krüger M, Scherer P, Brixius K, Schwinger RH, Pfitzer G. Isometric force kinetics upon rapid activation and relaxation of mouse, guinea pig and human heart muscle studied on the subcellular myofibrillar level. Basic Res Cardiol. 97Suppl 1:I127-35, 2002.
14. Tesi C, Piroddi N, Colomo F, PoggesiC.Relaxation kinetics following sudden Ca(2+) reduction in single myofibrils from skeletal muscle. Biophys J. 83(4):2142-51, 2002.
15. terKeurs HE. The interaction of Ca2+ with sarcomeric proteins: role in function and dysfunction of the heart. Am J Physiol Heart Circ Physiol. 1;302(1):H38-50, 2012.
16. Leu NA., Kurosaka S and Kashina A. Conditional Tek promoter-driven deletion of arginyltransferase in the germ line causes defects in gametogenesis and early embryonic lethality in mice. PLoSOne 4, e7734, 2009.
17. Kurosaka S, Leu NA, Zhang F, Bunte R, Saha S, Wang J, Guo C, He W, Kashina A.Arginylation-dependent neural crest cell migration is essential for mouse development. PLoS Genet 6, e1000878, 2010.
18. Agah R, Frenkel PA, French BA, Michael LH, Overbeek PA, Schneider MD. Gene recombination in postmitotic cells. Targeted expression of Crerecombinase provokes cardiac-restricted, site-specific rearrangement in adult ventricular muscle in vivo. J Clin Invest 100:169-179,1997.
19. Rai R, Wong CC, Xu T, Leu NA, Dong DW, Guo C, McLaughlin KJ, Yates JR 3rd, Kashina A. Arginyltransferase regulates alpha cardiac actin function, myofibril formation and contractility during heart development. Development 135:3881-3889, 2008.
20. Rassier DE, Pavlov I. Contractile characteristics of sarcomeres arrengedind series or mechanically isolated from myofibrils. Adv Exp Med Biol, 682:123-40, 2010.
21. Piroddi N, Belus A, Scellini B, Tesi C, Giunti G, Cerbai E, Mugelli A, Poggesi C. Tension generation and relaxation in single myofibrils from human atrial and ventricular myocardium. Pflugers Arch. 454(1):63-73, 2007.
22. Makarenko I, Opitz CA, Leake MC, Neagoe C, Kulke M, Gwathmey JK, del Monte F, Hajjar RJ, Linke WA. Passive stiffness changes caused by up regulation of compliant titin isoforms in human dilated cardiomyopathy hearts. Circ Res. 95:708-16, 2004.
23. Scellini B, Piroddi N, Poggesi C, Tesi C. Extraction and replacement of the tropomyosin-troponin complex in isolated myofibrils. Adv Exp Med Biol. 682:163-74: 2010.

24. Patel JR, Pleitner JM, Moss RL, Greaser ML. Magnitude of length-dependent changes in contractile properties varies with titin isoform in rat ventricles. Am J Physiol Heart CircPhysiol 302:H697-708, 2012.
25. Neagoe C, Kulke M, del Monte F, Gwathmey JK, de Tombe PP, Hajjar RJ, Linke WA.et al. Titin isoform switch in ischemic human heart disease. *Circulation* 106: 1333-1341, 2002.
26. Fridén J, Lieber RL. Spasticmuscle cells are shorter and stiffer than normal cells. Muscle Nerve. 27:157-64, 2003.
27. Warren CM, Jordan MC, Roos KP, Krzesinski PR, Greaser ML. Titin isoform expression in normal and hypertensive myocardium. Cardiovasc Res. 1;59(1):86-94, 2003.
28. Ottenheijm CAC, Granzier H. Role of titin in skeletal muscle function and disease. In: Muscle Biophysics: from molecules to cells. AdvExperim Med Biol, v. 682, 2010.
29. van Hees HW, Schellekens WJ, Andrade Acuña GL, Linkels M, Hafmans T, Ottenheijm CA, Granzier HL, Scheffer GJ, van der Hoeven JG, Dekhuijzen PN, Heunks LM. Titin and diaphragm dysfunction in mechanically ventilated rats. IntensiveCare Med. 38(4):702-9, 2012.
30. Nagueh SF, Shah G, Wu Y, Torre-Amione G, King NM, Lahmers S, Witt CC, Becker K, Labeit S, Granzier HL. Altered titin expression, myocardial stiffness, and left ventricular function in patients with dilated cardiomyopathy. Circulation. 13: 110 (2): 155-62, 2004.
31. Granzier H, Wu Y, Siegfried L, LeWinter M. Titin: physiological function and role in cardiomyopathy and failure. Heart Fail Rev.10(3):211-23, 2005.

ARTIGO III

Contractile properties of diaphragm myofibrils isolated from mice with heart-specific deletion of arginyl-tRNA-protein transferase

Propriedades contráteis de miofibrilas isoladas de diafragma de camundongos com knockout cardíaco específico para arginil-transferase

Contractile properties of diaphragm myofibrils isolated from mice with heart-specific deletion of arginyl-tRNA-protein transferase

Paula A. B. Ribeiro[1], Jorge P. Ribeiro[1], Fábio C. Minozzo[2], Ivan Pavlov[2], Nicolae Adrian Leu[3], Satoshi Kurosaka[3], Anna Kashina[3], Dilson E. Rassier[2,4, 5]

[1] Exercise Pathophysiology Research Laboratory and Cardiology Division, Hospital de Clínicas de Porto Alegre ; Faculty of Medicine, Federal Universityh of Rio Grande do Sul, Porto Alegre, Brazil;
[2] Department of Kinesiology, McGill University, Canada;
[3] Department of Animal Biology, School of Veterinary Medicine, University of Pennsylvania, USA
[4] Department of Physics and Physiology, McGill University, Canada;
[5] Meakins-Christie Laboratories, McGill University, Montreal, QC, Canada.

Abstract

Background: A mouse model with cardiomyocyte specific to arginyl-tRNA-protein transferase α-MHC knockout mice (α-MHC Ate1CKO), which presents dilated cardiomyopathy, and reduced heart contractile force, develops chronic heart failure (CHF). In humans, CHF may be accompanied of inspiratory muscle weakness but is not clear yet if this condition comes from impaired contractile properties of diaphragm. To test the hypothesis α-MHC Ate1CKO mice CHF is associated with abnormal contractile properties of the diaphragm, we used a newly developed system to work with isolated diaphragm myofibrils. Diaphragms from 6 α-MHC Ate 1 CKO mice and 6 age-matched wild type (WT) mice were used in our experiments. Myofibrils bundles were attached to an atomic force cantilever system, which was used for force measurements during activation/deactivation cycles. Active and passive forces at sarcomere lengths (SL) between 2.2 and 3.0 μm were measured. The maximal isometric forces were higher in α-MHC Ate1 CKO myofibrils (208.7 ± 30.7 nN/μm^2) than in WT myofibrils (122.8 ± 19.9nN/μm^2). There were no differences between the passive forces. The rate of force development (K_{act}) was similar between groups (α-MHC Ate1 CKO: 3.54 ± 0.37 sec^{-1}, WT: 2.78 ± 0.29 sec^{-1}). The rates of relaxation upon muscle deactivation (K_{rel}) were different between groups (Ate1 CKO: 6.11 ± 0.41 sec^{-1}, WT: 4.63 ± 0.41 sec^{-1}), suggesting a delay on relaxation in α-MHC Ate1 CKO myofibrils. Contrary to our working hypothesis, these results imply that diaphragm myofibrils from Ate 1 CKO mice produce an increased force. While the mechanisms need investigation, they suggest a potential compensatory mechanism by which the diaphragm works under loading conditions in α-MHC Ate1 CKO cardiomyopathy.

Heart failure; diaphragm; myofibrils; sarcomere, myosin, Ate 1 CKO.

Introduction

Chronic heart failure (CHF) is frequently associated with skeletal muscle involvement, including peripheral and inspiratory muscles[1]. Inspiratory muscle weakness (IMW) may be present in more than 30 % of patients in specialized heart failure clinics, and has important impact in functional capacity, quality of life, and prognosis[2]. The mechanisms responsible for IMW have not been fully elucidated. On one hand, van Hees et al.[3] observed that single fibers isolated from the diaphragm in rats with CHF presented a reduction in force and myosin heavy chain (MHC). On the other hand, a study using whole, intact diaphragm muscle failed to observe a reduction in tolerance to fatigue in CHF[4].

We have recently developed a mouse model with cardiomyocyte-specific to arginyl-tRNA-protein transferase knockout. The mice had a highly specific, conditional deletion of *Ate1* driven by α-myosin heavy chain promoter (α-MHC-*Ate1*CKO), which leads to cardiomyophathy and CHF[5]. Isolated myofibrils of these mice present marked abnormal contractile proteins and passive structures within sarcomeres (Ribeiro et al. unpublished data). The advantage of using these

CKO mice is that, unlikely other experimental models, cardiomyophathy is caused by specific deletion of *Ate1* in the heart, which inhibits protein arginylation catalyzed by Ate1, but has no direct effects on skeletal muscles[5]. Therefore, this model may be particularly suited for the evaluation of the involvement of inspiratory muscles in cardiomyopathy.

In the present study, the use of myofibrils allows the investigation of the smallest contractile unit of the diaphragm – the sarcomeres – and thus confounding effects from other cellular and extracellular sources (e.g. excitation-contraction coupling, action potential conduction, muscle membrane) are avoided. To test the hypothesis that diaphragm contractile properties are affected in the mouse model with α-MHC Ate1CKO which leads to CHF, we conducted the present study.

Methods

Six mice with heart-specific deletion of arginyl-tRNA-protein transferase (Ate 1) and six age-matched wild type mice (WT) were used in this study. The animals were older than 1 year (mean= 461±40 days) which corresponds to elderly in humans. Mice were euthanized and dissected to assess the chest cavity for diaphragm extraction. Our previous study showed that those animals presented higher mortality than WT, higher heart to body weight ratio, and accumulation of effusion in the thoracic and abdominal cavity, compatible with congestive heart failure[5].

Experiments and preparation for analysis of mechanical properties were conducted as earlier described[5]. Shortly, after diaphragm muscles extraction, from WT and Ate1 CKO mice, they were stored in rigor solution. On the day of the experiments, small pieces of the samples were homogenized following standard procedures[6], which resulted in a solution containing small bundles of myofibrils.

The myofibrils were transferred to the experimental setup. Small bundles of 4 to 15 myofibrils were chosen for mechanical testing, based on striation pattern and number of sarcomeres in series (between 10 and 30). Using micromanipulators, myofibrils were attached between atomic force cantilevers (AFC) and a glass needle. A computer-controlled system for activation/deactivation of the myofibrils was used (relaxing pCa^{2+} 9.0, activating pCa^{2+} 4.5). Length changes during the experiments were induced with a piezo motor. Under high magnification the contrast between the dark bands of myosin (A-bands) and the light bands of actin (I-bands) provided a dark-light intensity pattern, representing the striation pattern produced by the sarcomeres, which allowed measurements of sarcomere length during the experiments. The cantilever deflection was detected and recorded using a newly developed optical system that allows for high time-resolution measurements of mechanical properties of myofibrils. Since we had the stiffness of the AFC (K) and the amount of cantilever displacement produced by the contraction (Δd), the force (F) could be calculated as $F = K \bullet \Delta d$.

Measurements of active and passive myofibril forces. Once the myofibrils were attached to the AFC and microneedles, they were adjusted to

average sarcomere lengths (SL) of 2.2 µm, 2.4 µm, 2.6 µm, 2.8 µm or 3.0 µm, in random order, to test the length dependence of active force production. The solution surrounding the myofibrils was chaged from pCa^{2+} 9.0 to pCa^{2+} 4.5, which caused activation and force development. Once the myofibrils were fully activated and maximal force was obtained, they underwent a shortening-stretching protocol (amplitude 30% SL; speed 10 µm/sec; interval between length changes 5 ms) during which the force declined and rapidly re-developed to reach a new steady state. This protocol was performed to access if the myofibrils were not damaged during the experiments. If they were, the force would not recover to similar levels after a quick stretch. On the other hand, a single stretch (i.e. without a preceding shortening) would change the length of the myofibril during the contraction. After the myofibrils were tested for active force at all SLs, they were tested for passive forces; the myofibrils were stretched passively (pCa^{2+} 9.0) in consecutive steps of 0.2 µm/sarcomere at a speed of 10 µm/sec starting from a SL of 1.8 µm to a SL of 3.0µm.

Data analysis. The maximal force produced by the diaphragm myofibrils was calculated after force development stabilization and after force redevelopment following the shortening-stretch protocol. This maneuver was used in order to test the myofibrils health. Forces were averaged for a period of 2s to avoid potential effects of artifact interfering with measured values. The passive forces produced by myofibrils during the step protocol were calculated after the stretches, when the force was stabilized in every new SL. All forces were normalized by the myofibril cross sectional area (CSA) and the number of the myofibrils, assuming circular geometry (average CSA = $1.5\mu m^2$). For each contraction, we analyzed the rate of force development (K_{act}) with a two-exponential equation (a*(1-exp(-k*t)-exp(-l*t))+b). For the rate of exponential relaxation following myofibril deactivation (K_{rel}), we fitted the data with a single-exponential equation (a*exp(-k*(t-c))+b). For both equations, F is force, t is time, K_1 and K_2 are rate constants for force development, a is the amplitude of the exponential(s), and b is the initial force value. Myofibril contractions were excluded from analysis if control forces during the experiment decreased by ≥20% of maximal force production.

Statistics. The variables with normal distribution were presented as mean ± standard error. Those variables without normal distribution were expressed as geometric mean and confidence intervals and transformed to Log_{10}. The comparisons between two groups were performed using ANOVA-two way for repeated measures. Multiple comparisons were performed using the Bonferroni correction. An analysis of outliers excluded data from further analyses when there were signs of myofibril damage. A significance of $p<0.05$ was adopted.

Results

Active and passive forces. Figure 1 shows contractions produced during a typical experiment conducted with myofibrils isolated from a diaphragm WT and CKO. During activation, force increased rapidly (K_{act}) and reached a

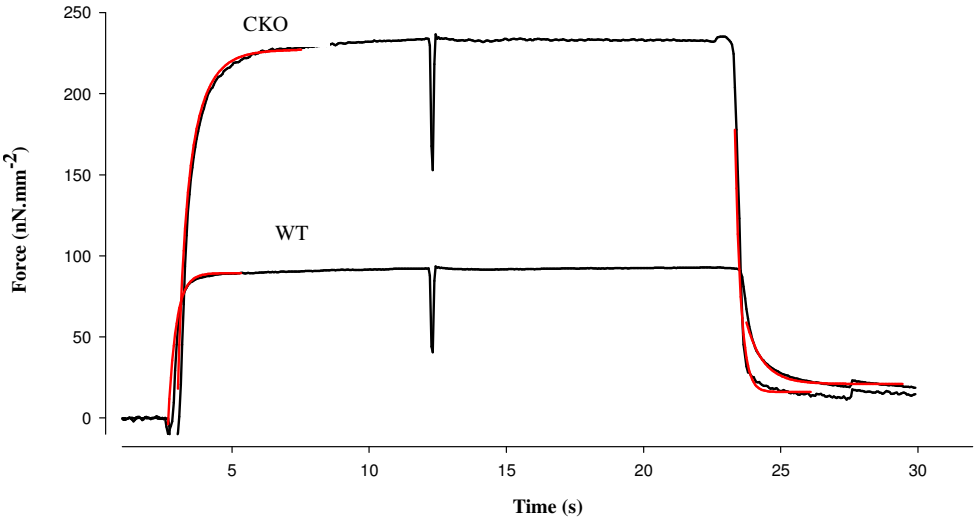

Figure 1. Typical data for α MHC Ate1 knockout (CKO) and wild type (WT) myofibrils maximal contraction. Red lines represent the fittings for rate of force development (K_{act}) and rate of relaxation (K_{rel}).

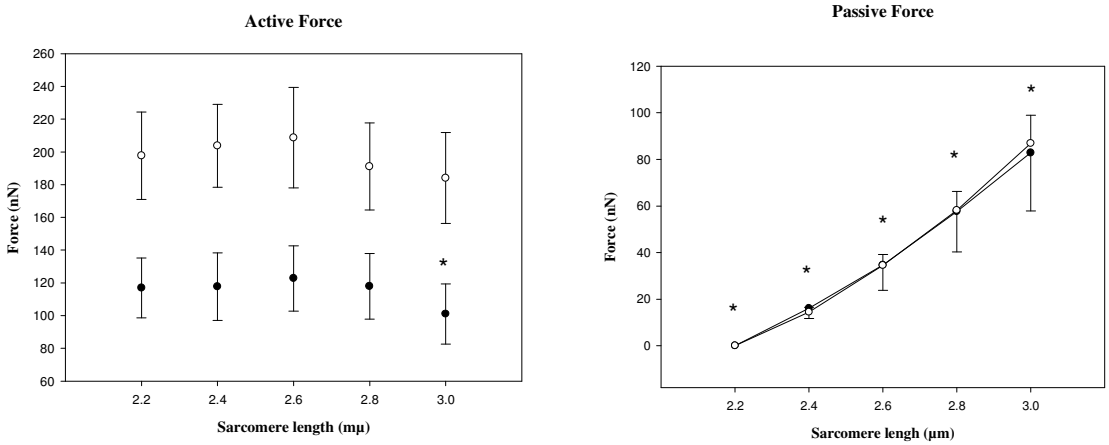

Figure 2. Panel A – Forces per cross sectional area at different sarcomere lengths for wild type (WT) and α MHC Ate1 knockout myofibrils (CKO). * All SL are different from 3.0. Panel B – Passive force for different sarcomere lengths for WT and KO myofibrils. * There is difference within all SL.

steady-state level. The maximal force produced by the Ate1 CKO was higher than the force produced by WT myofibril and, in this example, it was more than double higher than the control force.

Figure 2 – panel A shows that α-MHC Ate1 CKO myofibrils produced 173.8 ± 23.9 nN/ μm^2 of force while the WT myofibrils produced 85.1 ± 17 nN/μm^2 of force during full activation. When compared to repeated measures there was a difference between groups (p=0.01) and for SL (<0.001), but no interaction. All SL were different from 3.0 μm SL. Figure2 - panel B shows the results of the step protocol with consecutive passive stretches (pCa^{2+} 9.0). Each stretch resulted in an increase in passive forces (WT and CKO p=0.001 for SL). Myofibrils isolated from Ate1 CKO muscles produced an increase in force that was similar to WT myofibrils.

Rates of development and relaxation. As shown in panel A of Figure 3, the

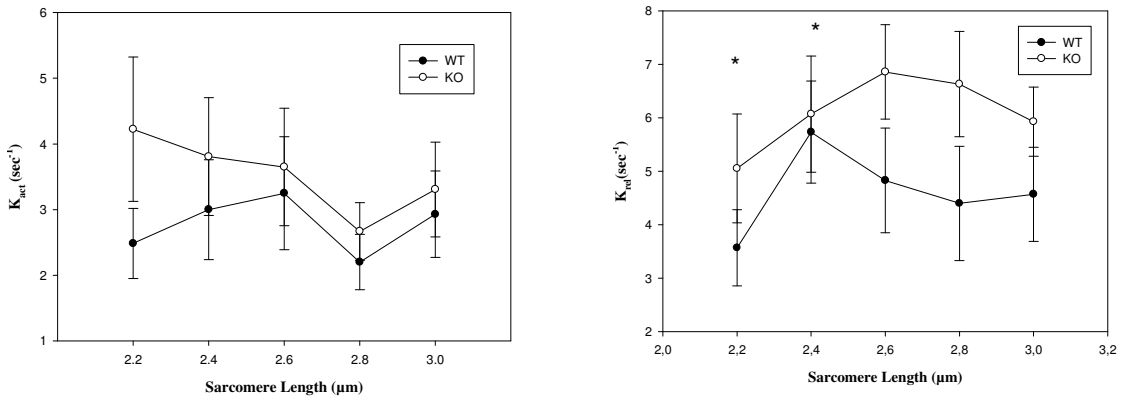

Figure 3: Panel A – Rate of force development (Kact) for different sarcomere lengths for wild type (WT) and α MHC Ate1 knockout (CKO) myofibrils. Panel B – Rate of relaxation (Krel) for different sarcomere lengths for WT and CKO myofibrils. There is difference between 2.2 and 2.4 SL.

values for K_{act} were similar between the two groups (Ate1 CKO: 3.54 ± 0.37 sec^{-1}, WT: 2.78 ± 0.29 sec^{-1}; p=0.25), and were not changed by length (p=0.24). In panel B of Figure 3, when groups were compared, K_{rel} was faster in the Ate1CKO then WT group (p=0.035), and influenced by sarcomere length (p=0.036, difference between 2.2 X 2.4 SL).

Discussion

The main purpose of this study was to assess mechanical properties of diaphragm contraction in α-MHC Ate 1 CKO mice, an animal model for human cardiomyopathy[5]. Contrary to our working hypothesis, our results showed an increase in active force production in the myofibrils from α-MHC Ate 1 CKO mice, while we failed to detect any differences in passive forces. These results indicate that this cardiomyophathy does not alter the contractile properties of the diaphragm. If anything, it is associated with increased contractile force.

Although the increase in the force of the diaphragm in α-MHC Ate 1 CKO myofibrils was unexpected, there is controversy in the literature regarding the effects of cardiomyophathy on skeletal muscle, and specifically the diaphragm. Tikunov et al.[7] investigated protein content in diaphragm isolated from humans with CHF and showed that the force of fibers containing predominantly MHC I was increased while the force in fibers containing predominantly MHC IIB was decreased. A subsequent study using single muscle fibers isolated from rats with CHF (caused by a ligation of the left coronary artery), showed that the force normalized per MHC content was not changed[3]. In fact, the force produced by fibers with a predominance of MHC I and MHC IIa was slightly increased in rats with CHF.

A maintenance (or increase) in diaphragm force in CHF is also in accordance with studies investigating other types of skeletal muscles[8, 9]. In a comprehensive study that analysed the vastus lateralis muscle from CHF patients and controls matched for age and physical activity level, there was

reduced force in MHC I fibers, but no differences in MHC IIA fibers[10]. These results suggest that, although there may be selective myosin depletion in skeletal muscles because of diseases, the force per contractile unit does not necessarily change, as also shown in cancer[11] and acute quadriplegic myopathy[12].

Our results do not allow us to understand the mechanisms by which the force in the diaphragms from α-MHC Ate 1 CKO myofibrils was increased. However, it is tempting to speculate that increased respiratory work in CHF may lead to a compensatory adaptation in the diaphragm[4]. Since the K_{act} was not altered in these myofibrils, the mechanisms for such compensation are not likely associated with changes in kinetics of myosin cross-bridges transiting between weakly bound and strongly bound states. Furthermore, the lack of differences in K_{act} suggests that the myofibrils were similar on their MHC distribution, i.e. a predominance of fast or slow MHC would have changed K_{act} accordingly[13]. The difference between groups in K_{rel} may be influenced by the higher number of cross-bridges on maximal contraction in α-MHC Ate 1 CKO[14]. Although our results suggest that MHC isoforms were not significantly different, this possibility needs to be tested in the future. However, analysis of MHC isoforms in isolated myofibrils is currently unfeasible.

If the α-MHC Ate1 CKO mice cardiomyopathy model has similarities with the presentation of chronic heart failure in humans, the findings of the present study, of a higher contractile function of the diaphragm, are in disagreement with the clinical presentation of inspiratory muscle weakness frequently found in CHF[1]. Patients with CHF present reduced inspiratory muscle strength and reduced inspiratory muscle endurance, as demonstrated by volitional tests[15, 16]. We have previously shown that inspiratory muscle training improves inspiratory muscle strength and endurance in this population, and the changes in inspiratory muscles strength correlate with hypertrophy of the diaphragm[15]. Therefore, the findings of the present study, of increased force generated by myofibrils, suggest that an adaptation in molecular mechanisms of force production per myofibril may compensate reduced number of myofibrils per fiber. MacFarlane et al[17] stimulated diaphragm fibers from habbits with heart failure using electrical and calcium stimulation. They showed augmented force generation in low frequencies, while high frequencies reduced force generation. Together with our data, these findings are consistent with the hypothesis inspiratory weakness in CHF may be secondary to calcium regulation or motorneuron activation, instead of myofibril contractility.

In conclusion, contrary to our working hypothesis, we found that the myofibrils from α-MHC Ate1CKO mice have higher active force and no impairment on passive force. Regardless of the mechanism by which cardiomyopathy is associated with an increase in the diaphragm strength it may represent an important and necessary mechanism to maintain normal respiratory function in cardiomyopathy.

Acknowledgements

The authors would like to acknowledge financial support from the Canadian Institutes for Health Research (CIHR), Fonds de Recherche du Québec – Nature et technologies (FRQNT), CAPES and CNPq (Brazil).

Disclosure of interest

The authors declare that they have no conflicts of interest concerning this article.

Author Contributions

Conceived and designed the experiments: PABR, DER, AK. Performed the experiments: PABR, IP. Analyzed data: PABR, FCM, DER, JPR. Wrote the paper: PABR, JPR, DER, FCM. Final review: AK, DER, JPR.

References

1. Ribeiro JP; Chiappa GR; Neder; JA; Frankenstein L. Respiratory muscle function and exercise intolerance in heart failure. Curr Heart Fail Rep. 6:95-101, 2009.

2. Dall'Ago P; Chiappa GR; Guths H; Stein R; Ribeiro JP. Inspiratory muscle training in patients with heart failure and inspiratory muscle weakness: a randomized trial. J Am Coll Cardiol. 47: 757-63, 2006.

3. 3.van Hees HWH; van der Heijden HFM; Ottenheijm CAC; Heunks LMA; Pigmans CJC; Verheugt FWA; Brouwer RMHJ; Dekhuijzen PNR. Diaphragm single-fiber weakness and loss of myosin in congestive heart failure rats. Am J Physiol Heart Circ Physiol, 293:H819-H828, 2007.

4. Mancini DM; Henson D; LaManca J; Levine S. Respiratory muscle function and dyspnea in patients with chronic congestive heart failure. Circulation. 86:909-18, 1992.

5. Kurosaka S; Leu NA; Pavlov I; Han X; Ribeiro PA; Xu T; Bunte R; Saha S; Wang J; Cornachione A; Mai W; Yates JR 3rd; Rassier DE; Kashina A. Arginylation regulates myofibrils to maintain heart function and prevent dilated cardiomyopathy. J Mol Cell Cardiol. 2012 May 21. [Epub ahead of print]

6. Rassier DE; Pavlov I. Contractile characteristics of sarcomeres arrenged ind series or mechanically isolated from myofibrils. Adv Exp Med Biol, 682:123-40, 2010.

7. Tikunov BA; Mancini D; Levine S. Changes in Myofibrillar protein composition of human diaphragm elicited by congestive heart failure. J Mol Cell Cardiol 28: 2537-2541, 1996.

8. De Sousa E; Veksler V; Bigard X; Mateo P; Ventura-Clapier R. Heart failure affects mitochondrial but not myofibrillar intrinsic properties of skeletal muscle. Circulation, 102:1847-53, 2000.

9. Okada Y; Toth MJ; VanBuren P. Skeletal muscle contractile protein function is preserved in human heart failure. J Appl Physiol 104:952-957, 2008.

10. Miller MS; Vanburen P; Lewinter MM; Lecker SH; Selby DE; Palmer BM; Maughan DW; Ades PA; Toth MJ. Mechanisms underlying skeletal muscle weakness in human heart failure: alterations in single fiber myosin protein content and function. Circ Heart Fail. 2:700-6, 2009.

11. Acharyya S; Ladner KJ; Nelsen LL; Damrauer J; Reiser PJ; Swoap S; Guttridge DC. Cancer cachexia is regulated by selective targeting of skeletal muscle gene products. J Clin Invest. 114:370-8, 2004.

12. Larsson L; Li X; Edström L; Eriksson LI; Zackrisson H; Argentini C; Schiaffino S. Acute quadriplegia and loss of muscle myosin in patients treated with nondepolarizing neuromuscular blocking agents and corticosteroids: mechanisms at the cellular and molecular levels. Crit Care Med. 28:34-45, 2000.

13. Bottinelli R; Reggiani C. Human skeletal muscle fibres: molecular and functional diversity. Prog Biophys Mol Biol. 73:195-262; 2000.

14. Stehle R; Solzin J; Iorga B; Poggesi C. Insights into the kinetics of Ca2+-regulated contraction and relaxation from myofibril studies. Pflugers Arch.458:337-57, 2009.

15. Chiappa GR; Roseguini BT; Vieira PJ; Alves CN; et al. Inspiratory muscle training improves distribution of blood flow to resting and exercising limbs in patients with chronic heart failure. J Am Coll Cardiol. 51:1663-71, 2008.

16. Winkelmann E; Chiappa GR; Lima COC; Viecili PRN; Stein R; Ribeiro JP. Addition of Inspiratory Muscle Training to Aerobic Training Improves Cardiorespiratory Responses to Exercise in Patients with Heart Failure and Inspiratory Muscle Weakness. The American Heart Journal, 158: 768.e1-768.e7, 2009.

17. MacFarlane NG; Darnley M; Smith GL. Cellular basis for contractile dysfunction in the diaphragm from a rabbit infarct model of heart failure. Am J Physiol Cell Physiol 278:C739-C746, 2000.

6. CONCLUSÕES:

I. Menos de 50 % da variância da força muscular inspiratória e da musculatura esquelética periférica pode ser explicada por variáveis clínicas e comportamentais de pacientes com insuficiência cardíaca crônica.

II. A variância da força muscular inspiratória, em pacientes com disfunção sistólica, pode ser explicada em 50% pela capacidade funcional dos pacientes.

III. Os achados biofísicos em músculo cardíaco de camundongos com knockout cardio-específico para arginilação são coerente com encontrados em humanos com insuficiência cardíaca.

IV. O aumento da contratilidade das miofibrilas do diafragma, no modelo de insuficiência cardíaca por knockout cardio-especifico para arginilação, sugere que a fraqueza muscular inspiratória não é secundária à disfunção contrátil da musculatura inspiratória.

V. Por fim, os mecanismos que levam a fraqueza muscular inspiratória ainda não se encontram totalmente elucidados. Estudos em humanos envolvendo mecanismos neurais e de atrofia devem ser conduzidos para maior compreensão dos mecanismos envolvidos nessa disfunção.

7. PRODUÇÃO CIENTÍFICA

Produção científica durante o doutorado no Brasil

1. Augmented peripheral chemoreflex in patients with heart failure and inspiratory muscle weakness. Callegaro CC, Martinez D, **Ribeiro PA**, Brod M, Ribeiro JP. Respir Physiol Neurobiol. 2010 Apr 15; 171 (1):31-5.

2. Physical activity advice only or structured exercise training and association with HbA1c levels in type 2 diabetes: a systematic review and meta-analysis. Umpierre D, **Ribeiro PA**, Kramer CK, Leitão CB, Zucatti AT, Azevedo MJ, Gross JL, Ribeiro JP, Schaan BD. JAMA. 2011 May 4;305(17):1790-9.

3. Volume of Supervised Exercise Training Impacts Glycemic Control in Patients with Type 2 Diabetes: A Systematic Review with Meta-Regression Analysis. D. Umpierre, **PA Ribeiro**, B.D. Schaan, J.P. Ribeiro (Submetido a Diabetologia).

4. Ventilatory and Metabolic Determinants of Self-Select Walking Speed in Heart Failure. Paula Figueiredo, **Paula A B Ribeiro**, Renata L Bona, Leonardo A Peyre-Tartaruga, Jorge P Ribeiro. (Submetido a Journal of Cardiac Failure).

Produção científica durante estágio sanduíche – McGill University

1. Arginylation in cardiomyocytes regulates myofibril properties to maintain heart function and prevent dilated cardiomyopathy. Satoshi Kurosaka, N. Adrian Leu, Ivan Pavlov, Xuemei Han, **Paula Aver Bretanha Ribeiro**, Tao Xu, Ralph Bunte, Sougata Saha, Wilfried Mai, John R Yates, Dilson E. Rassier, and Anna Kashina. Journal of Molecular Cell and Cardiology, 2012. Disponível on line.

Trabalhos apresentados em Congressos Internacionais

1. Ribeiro, P. A. B. ; Trevisol, F. S. ; Grigoletti, S. ; Ikeda, M. L. ; Fuchs, S. C. . Methodological Analysis of Accelerometry Measure of Physical Activity in HIV Patients. International Congress of Physical Activity and Public Health - Toronto : 2010.

2. Ribeiro, P. A. B. ; Trevisol, F. S. ; Reichert FF ; Grigoletti, S. ; Ferroni, L. ; Alencastro, P. R. ; Fuchs, S. C. . Comparison between IPAQ Classification and Number of Daily Steps among HIV Patients. 3thInternational Congress of Physical Activity and Public Health - Toronto : 2010.

3. Paula AB Ribeiro, Ivan Pavlov, Fabio Minozzo, Nicolae Adrian Leu, Satoshi Kurosaka, Anna Kashina, Dilson Rassier. Contractile properties of myocardium myofibrils isolated from mice with heart-specific deletion of arginyl-tRNA-protein transferase. 56th Annual Meeting Biophysical Society – San Diego: 2012.

Anexo 1:

8. DETALHAMENTO METODOLOGICO DOS ESTUDOS 2 E 3.

Devido a complexidade metodológica do estudo, neste capítulo apresentaremos a metodologia detalhada referente aos estudos 2 e 3, realizados sob orientação do Prof Dr. Dilson Rassier, no Muscle Physiology and Biophysics Laboratory, do Department of Kinesiology and Physical Education na McGill University.

8.1. Animais:

Para estes estudos foram usados camundongos knockout para arginilação. A arginilação pós-translacional é um mecanismo molecular não explorado que é crítico para o desenvolvimento cardíaco (Saha e Kashina, 2011). Camundongos "knockout" para arginilação apresentam a letalidade embriônica e problemas cardíacos que são similares aos que ocorrem em humanos. Resultados preliminares demonstraram que a ablação da arginilação no início do desenvolvimento resulta em defeitos ventriculares e do septo atrial, comumente observados em doenças congênitas humanas, incluindo a altamente destrutiva síndrome de DiGeorge. Estudos em desenvolvimento mostram que a depleção específica de arginyltransferase (Ate1) na diferenciação dos miócitos promove miocardiopatia dilatada e, por conseqüência, insuficiência cardíaca congestiva em camundongos, levando a letalidade pos-natal tardia com sintomas de insuficiência cardíaca relacionada ao envelhecimento (Kurosaka, et al. dados não publicados - Anexo 1).

8.2. Geração do camundongo knockout αMHC-*Ate1*.

Um modelo de camundongo para knockout da arginil transferase (Ate1) cardiomiócito especifico foi desenvolvido usando uma linhagem prévia de '*Ate1*-floxed' (Leu et al., 2009; Kurosaka et al., 2010), o qual foi cruzado com αMHC-Cre mice (Agah et al., 1997), o qual a Cre recombinase é expressa na forma do promotor de αmiosina de cadeia pesada que é ativada por diferenciação, resultando na deleção da *Ate1* no músculo cardíaco (camundongo αMHC-*Ate1*). Detalhes da geração do camundongo Ate 1 KO podem ser encontradas em Kurosaka et al. (2012 - Anexo 1). Os tecidos cardíacos e diafragmáticos foram extraídos e cedidos pela pesquisadora Dra. Anna Kashina da Pennsylvania University.

8.3. Amostras de tecido cardíaco e diafragmático:

As amostra de músculos cardíacos e diafragmas dos camundongos foram recebidas e armazenadas em solução Rigor/glicerol 1:1 (v/v) a -20ºC por 2 semanas (tabela 1). No dia do experimento, uma porção foi dissecada em pequenas peças de $2mm^3$ e homogeneizada em uma nova solução rigor utilizando um homogeinizador (VWR AHS250, Canada), a 24000 rpm/s; repetido por 3 vezes. A solução homogeneizada contém pequenos feixes de miofibrilas, a qual pode ser usada em vários experimentos.

	Rigor	pCa2+ 9,0	pCa2+ 4,5
NaCl	132	-	-
KCl	5	-	52,3
Glucose	7	-	-
$MgCl_2 \cdot 6H_2O$	1	-	5.4
$(CH_3COO)_2Mg \cdot 4H_2O$	-	2,5	-
THAM	4	-	-
EGTA	5	5	7
$CaCl_2$	-	-	7
Imidazole	-	-	20,56
Creatine Phostphate	-	-	18,82
MOPS	-	20	-
ATP	-	10	6,17
Kprop	-	170	-

Tabela 1. Solução (em mM) usada para os experimentos. O pH para toda solução será ajustado para pH 7.0 antes de cada experimento adicionando KOH ou HCl diretamente nas soluções. Todas as soluções continham inibidores de proteínas (*Roche Complete protease inhibitors, Roche Diagnostics)*, o qual inibe a ação da quimiotripsina, thermolisina, papaina, pronase e tripsina.

8.4. Protocolo Experimental

Aproximadamente 200 µL do homogeneizado foi adicionado ao experimento em banho com temperatura controlada (~10°C) contendo solução com pCa^{2+} 9,0. O banho foi ajustado em um microscópio invertido (Nikon TE-2000U), e foi mantido em

temperatura constante. O excesso de miofibrilas foi lavado com solução de relaxamento (baixa concentração de Ca^{2+}). Um feixe de miofibrilas (3-6 miofibrilas por feixe) foi selecionado, baseado na qualidade e consistência do padrão de estriamento. Usando micromanipuladores, as miofibrilas suspensas acima do fundo do banho foram fixadas em uma agulha rígida de vidro e um transdutor de forca atômica. A agulha de vidro tem rigidez maior que 2000 nN/µm. Os transdutores de força (modelo: ATEC-CONTPt) foram adquiridos da Nanosensors™ *(USA) com uma rigidez média de 0,2 N/m, variando de 0,02 a 0,75N/m.

Antes do uso, cada transdutor foi calibrado contra uma agulha de rigidez conhecida. Os transdutores foram colocados em contato com uma agulha rígida, a qual foi movida uma pequena distancia (~2 µm) causando uma deflecção de ambos, a alça e a agulha. Baseado na deflecção a rigidez pode ser calculada:

$$k_c = \frac{k_n \Delta d_n}{\Delta d_c}$$

onde k_n e k_c são a rigidez da agulha e da alça, respectivamente, Δd_n é o deslocamento da ponta da agulha, e Δd_c é o deslocamento da ponta da alça.

As miofibrilas foram fixadas na agulha rígida e na alça usando um adesivo (Dow Corning adhesive 3145 RTV - MIL-A-46146). A agulha posicionada em um braço piezo-acionado foi controlado por protocolos de rápido encurtamento e alongamento computadorizados. A adição de soluções foi realizada usando uma seqüência de pipetas, posicionadas em um sistema de perfusão de multicanais (VC-6M, Harvard Apparatus, USA). Nesse sistema, a solução de ativação é acionada por um lado de uma pipeta dupla, enquanto a solução de relaxamento é acionada pelo outro lado. Para evitar a mistura entre soluções, uma bomba peristáltica (Instech P720, Harvard Apparatus,

USA) estará continuamente removendo as soluções por um orifício oposto a ponta da pipeta dupla.

A força e o encurtamento produzidos pela miofibrilas causam deflecções na alça proporcionais a sua rigidez e a força gerada pela miofibrilas. Variações no ângulo da deflecção da luz do laser incidente na alça são registradas num detector de quatro quadrantes e usadas para determinar o deslocamento da alça e das forças produzidas pelas ativações das miofibrilas. Os valores das forças foram normalizados pela área transversal teórica estimada das amostras (~1,5μm^2).

O comprimento médio do sarcômero das miofibrilas suspensas foi medido antes do experimento, e ajustes passivos do comprimento foram realizados para obter o comprimento inicial do sarcômero de acordo com o experimento. As medidas de comprimento e as gravações das contrações foram realizadas sob magnificação de 90X (Nikon Plan Fluor 60X, N.A. 0.70), com adicional magnificação interna de 1,5X usando uma câmera CCD (Go-3, QImaging, USA; pixel size: 3,2 µm X 3,2 µm). Com o feixe de miofibrilas suspenso aproximadamente 50 µm acima do fundo da câmara, é realizada uma contração seguida por um rápido encurtamento e alongamento, finalizando com relaxamento da amostra. O ciclo encurtamento-alongamento é realizado para medidas da taxa de força redesenvolvida (*rate of force redevelopment* -k_{tr}), a qual fornece uma indicação de transição entre as pontes cruzadas conectadas à actina, de um estado prévio ao "power-stroke" a um estado de produção de forca. O encurtamento e o alongamento tiveram magnitudes semelhantes, com magnitude de 20% a 30% da medida do comprimento inicial das miofibrilas. Os intervalos de ativação, encurtamento – realongamento, e relaxamento foram de aproximadamente 30 segundos. Este procedimento será repetido 5 vezes em cada amostra quando possível, para avaliação da propriedades dependentes dos diferentes comprimentos de sarcômero. As amostras não

foram submetidas a ativações repetidas quando apresentaram dano significativo na ativação prévia.

8.5. Análise dos dados experimentais

As forças transientes inicialmente desenvolvidas e redesenvolvidas foram ajustadas em uma equação exponencial simples:

$$F = a(1 - e^{-ct}) + b \qquad \ldots (1)$$

onde F é força, t é tempo, c e d são taxas constantes para desenvolvimento de força, a é a amplitude do desenvolvimento de força exponencial na Eq. (1), b é o valor de força inicial. Ajustando as forças transientes para equações exponenciais nos permite determinar as taxas constantes para desenvolvimento e redesenvolvimento (k_{ACT} and k_{tr}, respectivamente). Forças transientes para fase relaxamento foram ajustadas a equação a seguir que inclui funções linear e exponencial:

$$F = (a + c)e^{-d(t-1)} + b \qquad \ldots (2)$$

onde F é força, c e d são taxas constantes de declínio de força, t é tempo, e b é a força de equilíbrio após relaxamento.

Referencias

Labuda A, Brastaviceanu T, Pavlov I, Paul W Rassier, D. Optical detection system for probing cantilever deflections parallel to a sample surface. Review of scientific instruments 82, 013701, 2011.

Anexo 2- suplemento

Kurosaka et al., "Arginylation regulates myofibrils to maintain heart function and prevent dilated cardiomyopathy" Supplemental Online Information.

Supplemental Figure 1. αMHC-*Ate1* (CKO) fetus with lac Z reporter to confirm that αMHC promoter-driven *Ate1* deletion was specific to the heart at E10.5 (E10.5, X-gal).

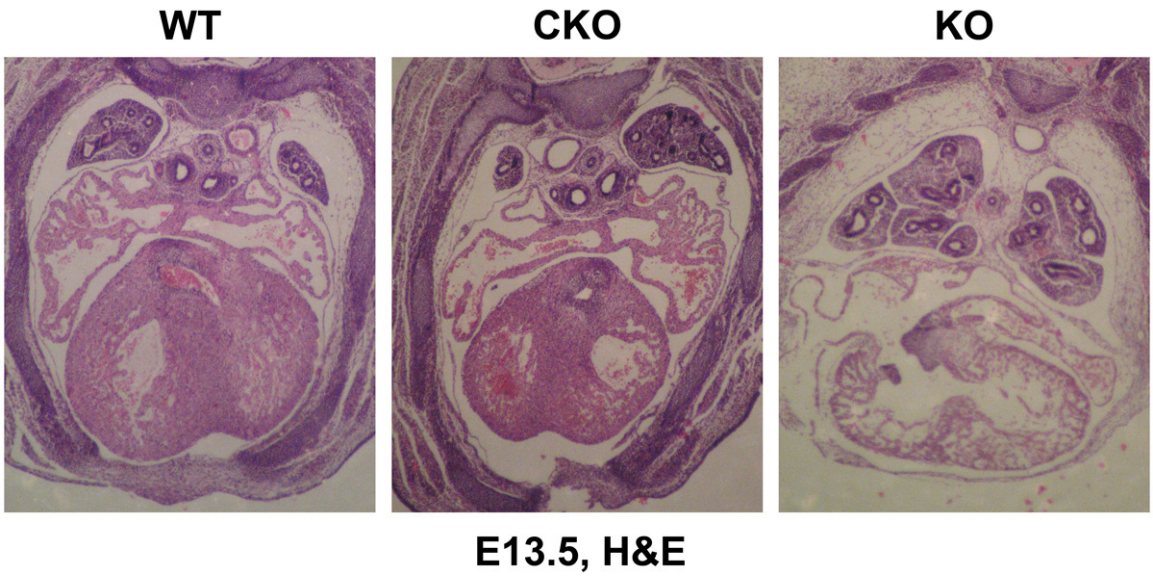

Supplemental Figure 2. Cross sections of mouse embryonic chest cavities at E13.5 stained with H &E. Wild type (WT) and CKO hearts have normal morphology, while *Ate1*$^{-/-}$ (KO) hearts shows severe defects.

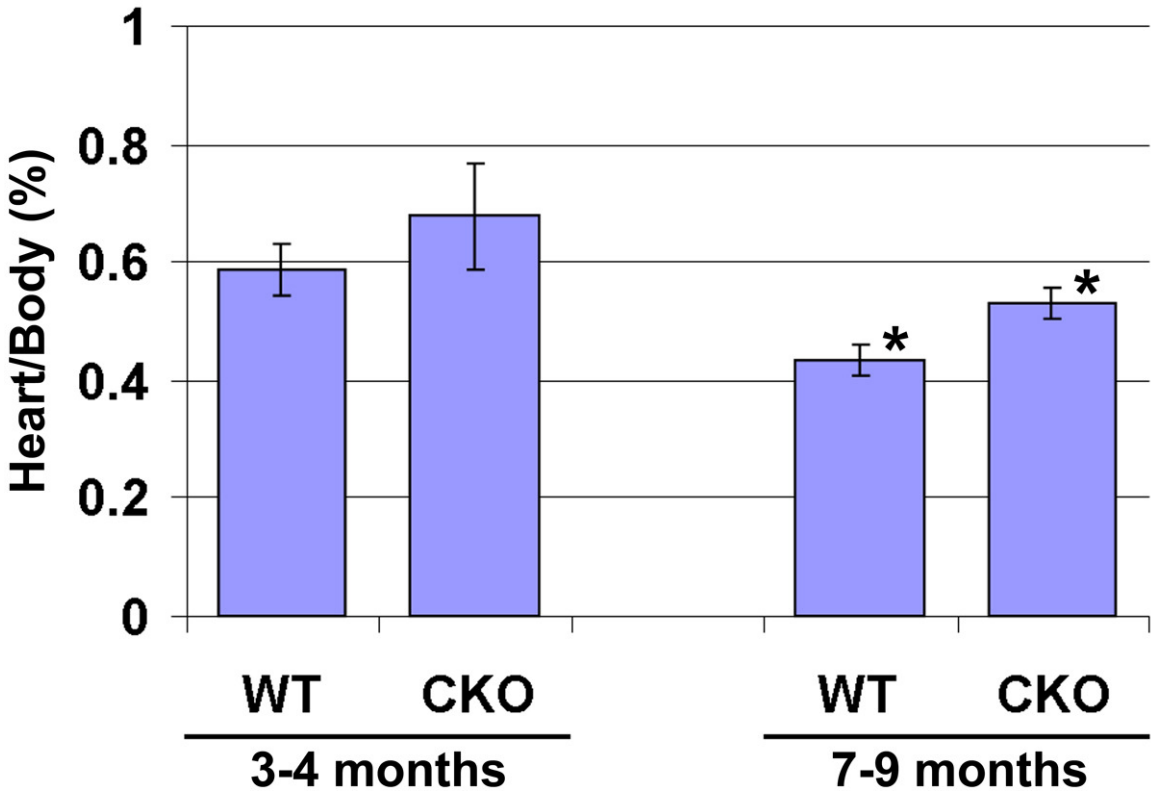

Supplemental Figure 3. Heart/Body ratio of mice at the ages of 3-4 months (p=0.40; WT: n=4; CKO: n=5) and 7-9 months (p=0.04; WT: n=4; CKO: n=5). Error bars represent SEM.

* represents significant difference (p<0.05) between columns.

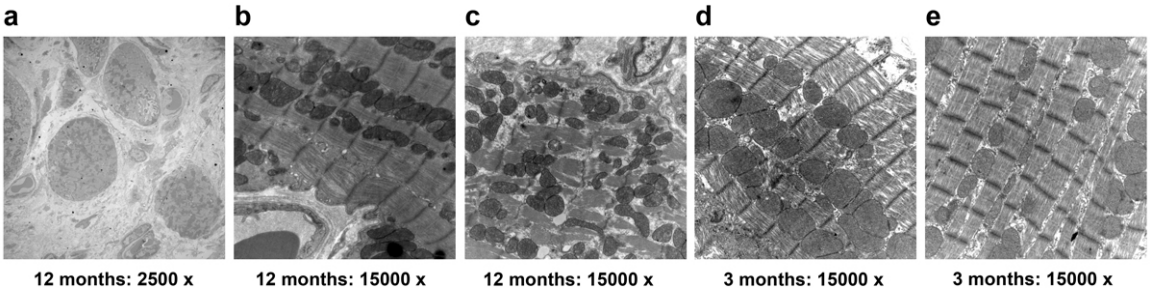

Supplemental Figure 4. Defective ultrastructures in CKO cardiomyocytes. (a) Cardiomyocytes appeared to be 'floating' in the extracellular matrix, rather than firmly connected to each other at 12 months (2500 x). (b) Miofibril structures were destroyed at 12 months (15000 x). (c) Sarcomere was broken (splitted) at 12 months (15000 x). (d) Destroyed sarcomeres at 3months (15000 x). (e) Diffused Z-bands at 3 months (15000 x).

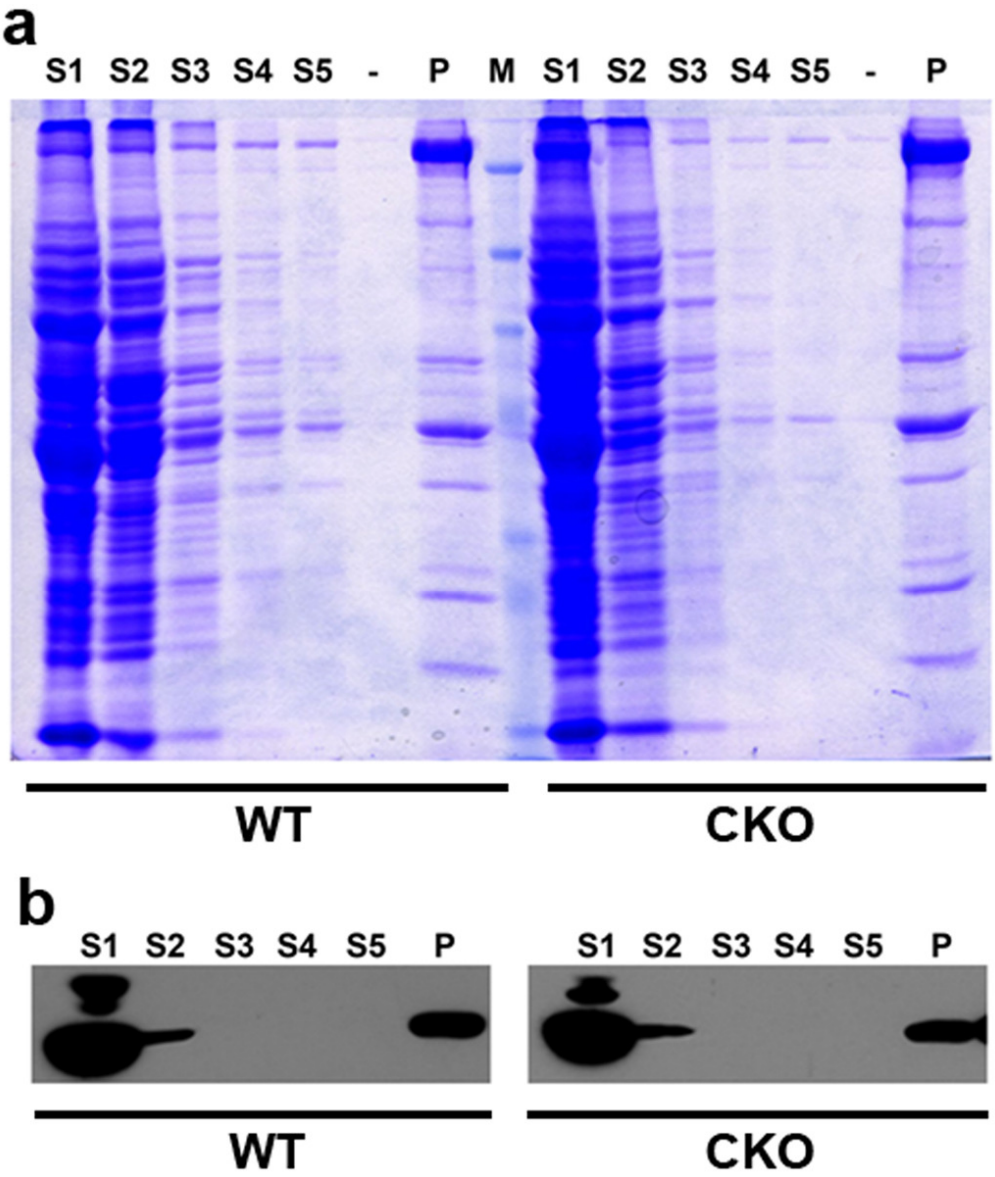

Supplemental Figure 5. Myofibrils (a) Coomassie blue staining of proteins in supernatants and myofibril pellets during the process of isolation of myofibrils. (b) Western blotting for actin in supernatants and myofibril pellets during the process of isolation of myofibrils. S1: supernatant after homogenization. S2: supernatant after Triton X-100 treatment. S3: supernatant after 1st wash. S4: supernatant after 2nd wash. S5: supernatant after 3rd wash. -: blank. P: pellet containing myofibrils.

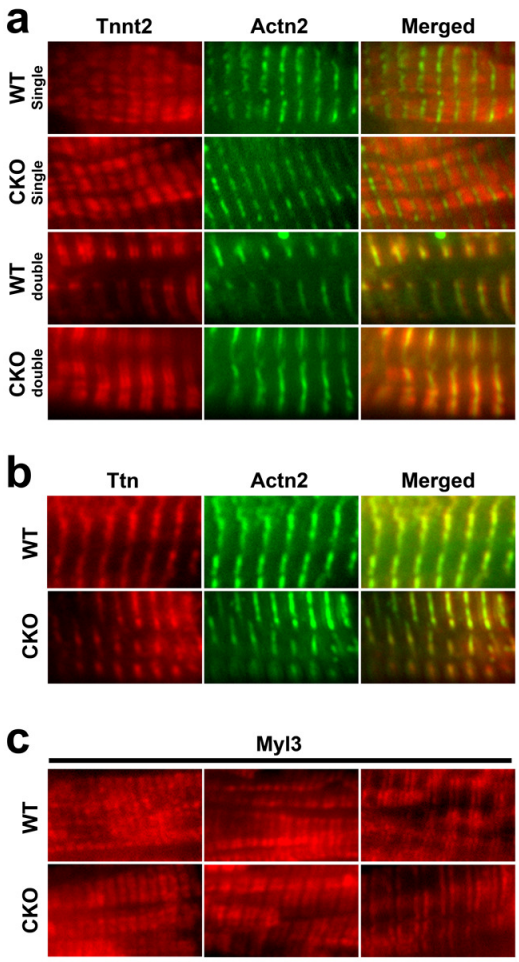

Supplemental Figure 6. (a) Alternating localization of cardiac troponin T2 (Tnnt2) and α-actinin 2 (Actn2) in cardiac myofibrils. Left panel; localization of Tnnt2; center panel: localization of Actn2; right panel: merged pictures (Merged); top row: Tnnt2 appears as single bands in WT mice; 2nd row: Tnnt2 appears as single bands in CKO mice; 3row: Tnnt2 appears as double bands in WT mice; bottom row: Tnnt2 appears as double bands in CKO mice. (b) Localization of titin (titin) and α-actinin 2 (Actn2) in cardiac myofibrils. Ttn (left panel) and Actn2 (center panel) are co-localized (Right panel) in both WT (top panel) and CKO (bottom panel). (c) Localization of myosin light chain 3 (Myl3) in WT (top panel) and CKO (bottom panel) mice.

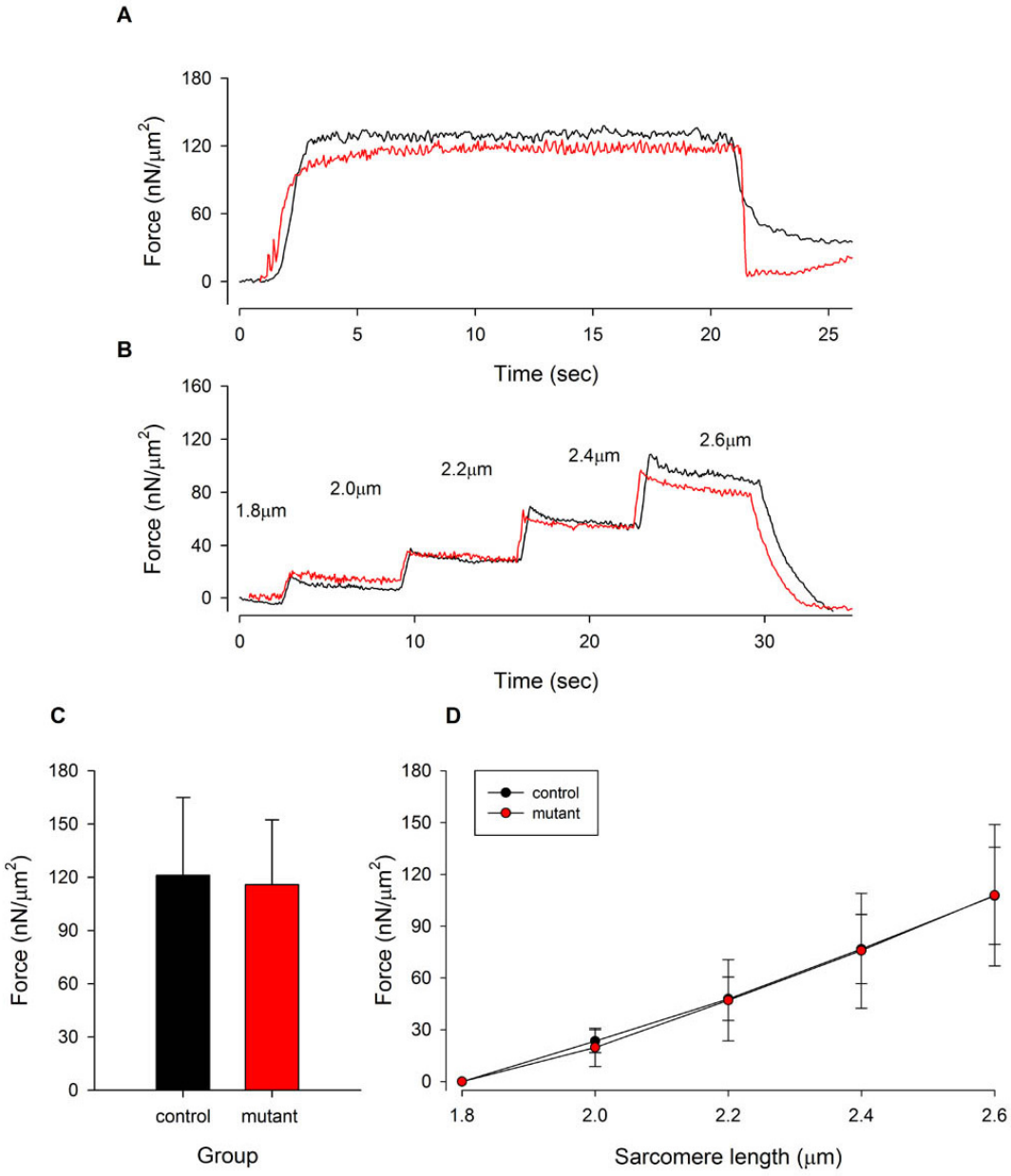

Supplemental Figure 7. Myofibril force measurements similar to those shown in Fig. 4 of the main text using younger (5-6 months old) mice. (a) Typical force measurements performed with two myofibril samples isolated from aged WT (black) and CKO (red) hearts. In both cases, myofibrils were activated at an initial SL of 2.2μm and after full activation the force was maintained stable until the myofibrils were relaxed. Note that the absolute force is significantly decreased in the mutant heart. (b) Consecutive stretches performed with non-activated myofibrils isolated from control (black) and mutant (red) hearts. Stretches were started at 1.8μm and were performed at magnitudes of 0.2μm at a speed of 10μm/1sec. Mean (± S.E.M.) values for (c) total active forces and (d) passive forces for myofibrils tested during these experiments. Multiple myofibrils from 4 age-matched control and αMHC-*Ate1* mice at 415 and 485 days old (2 pairs at each age) were analyzed.